Smart Agricultural Technology 12 (2025) 101203

Contents lists available at ScienceDirect

Smart Agricultural Technology

journal homepage: www.journals.elsevier.com/smart-agricultural-technology

Integration of agronomic information, vegetation indices (VIs), and meteorological data for phenological monitoring and yield estimation of rice (*Oryza sativa* L.)

Jorge A. Fernandez-Jibaja [a], Nilton Atalaya-Marin [a], Yeltsin A. Álvarez-Robledo [a], Victor H. Taboada-Mitma [a], Juancarlos Cruz-Luis [b], Daniel Tineo [a,*], Malluri Goñas [a], Darwin Gómez-Fernández [a]

[a] Centro Experimental Yanayacu, Dirección de Servicios Estratégicos Agrarios (DSEA), Instituto Nacional de Innovación Agraria (INIA), Carretera Jaén San Ignacio KM 23.7, Jaén 06801, Cajamarca, Peru
[b] Dirección de Servicios Estratégicos Agrarios (DSEA), Instituto Nacional de Innovación Agraria (INIA), Av. Molina 1981, Lima 15024, Peru

ARTICLE INFO

Keywords:
Agronomic traits
Crop monitoring
Meteorological information
Remote sensing
Rice yield estimation

ABSTRACT

Rice (*Oryza sativa* L.) is a staple crop for sustaining global food security and is particularly important in tropical and subtropical regions. In this context, precision agriculture enables more efficient crop management to increase productivity and sustainability. This study proposes an integrated framework for monitoring the phenological development and estimating the yield of *O. sativa* by combining agronomic variables, vegetation indices (VIs), and meteorological data. Six rice varieties (Victoria, Esperanza, Bellavista, Puntilla, Capoteña, and Valor) were evaluated across six phenological stages using field data, 20 VIs and meteorological parameters. Field data revealed greater tillering of the Puntilla and Valor varieties (9–28 tillers), with Esperanza having the most stable chlorophyll values (21.5–38.7, $\sigma = 10.46$) during ripening. The temporal dynamics of the VIs consistently increased from the seedling to inflorescence emergence stage, followed by a decrease during flowering and ripening, which aligns with known physiological transitions in rice, however, significant differences in the NDVI index were detected during ripening ($p > 0.05$). For yield estimation, feature selection was performed using principal component analysis (PCA) and the least absolute shrinkage and selection operator (LASSO) to increase model efficiency and interpretability. Among the regression algorithms tested, support vector regression (SVR) demonstrated the highest predictive accuracy ($R^2 = 0.81$) for the Bellavista variety at the maximum tillering stage. Furthermore, the Valor variety presented the highest grain yield (13.70 t/ha). These results underscore the potential of integrating multisource data with machine learning techniques for high-resolution phenological monitoring and varietal performance assessment.

1. Introduction

Rice is the third most widely produced crop worldwide and serves as a staple food for >3.5 billion people globally [1,2]. Global rice production has shown an increasing trend in recent decades, reaching 512.9 million tons in 2022 [1,3]. The leading rice-producing countries worldwide are China, India, and Indonesia [1,3]. Although Latin America and the Caribbean are not among the top rice-producing regions, rice remains the primary source of calories in many of the countries in these regions [4]. A specific case is Peru, where rice is a fundamental component of the basic food basket [1,4]; it ranks third in national agricultural production [1] placing the country among those with the highest average rice yields (8.4 t/ha) [5].

Rice demand has increased significantly worldwide, approaching the volume available in the market [3]. Demographic projections estimate that by 2050, the world population will reach 9.7 billion people [6] requiring a 70 % increase in rice production to meet global food demand [7]. At a more regional scale, Latin America and the Caribbean are expected to face complex socioeconomic scenarios [8]. Within this context, considering the growing global population and rice

* Corresponding author at: Centro Experimental Yanayacu, Dirección de Servicios Estratégicos Agrarios (DSEA), Instituto Nacional de Innovación Agraria (INIA), Carretera Jaén San Ignacio KM 23.7, Jaén 06801, Cajamarca, Peru.
E-mail address: dt.infolab@gmail.com (D. Tineo).

https://doi.org/10.1016/j.atech.2025.101203
Received 6 May 2025; Received in revised form 10 July 2025; Accepted 14 July 2025
Available online 15 July 2025

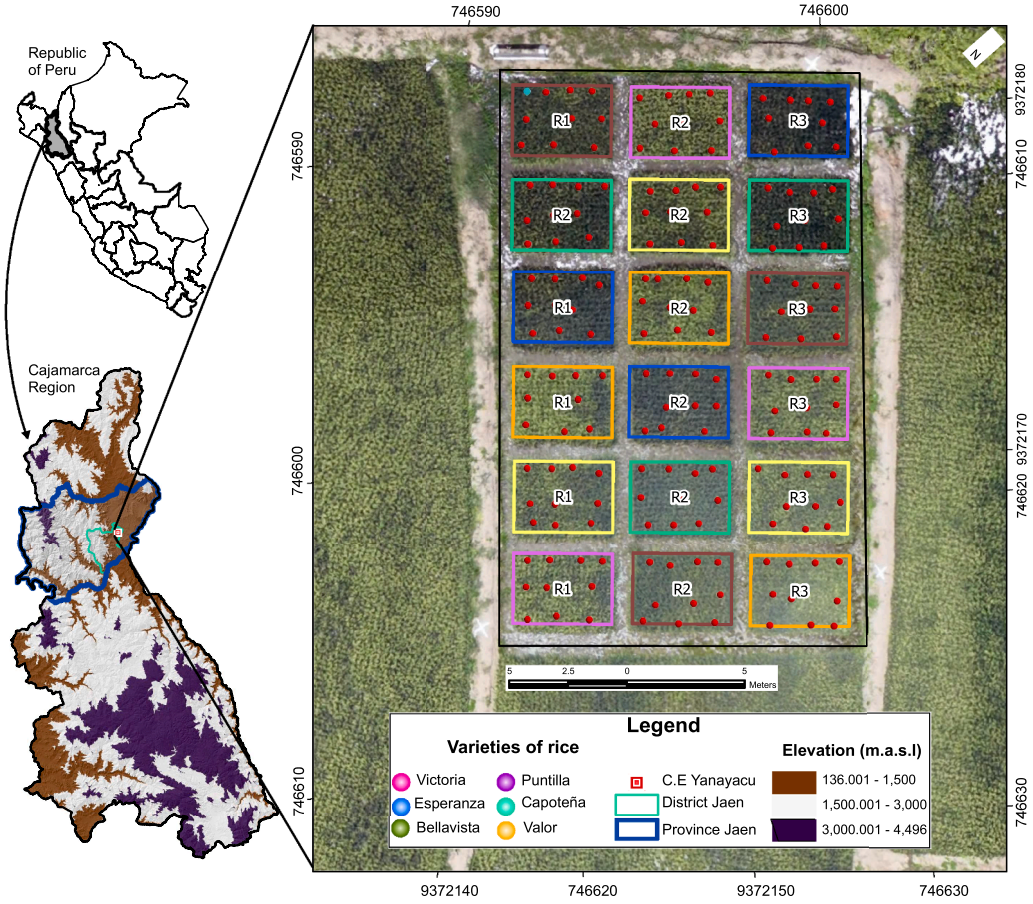

Fig. 1. Location of the experimental plot and design scheme at the Yanayacu Experimental Center, Jaén, Cajamarca, Peru.

consumption, ensuring the supply of this staple crop is essential for guaranteeing food security [9,10]. To address these challenges, two main strategies have been adopted: expanding agricultural land and increasing productivity indices. The latter approach depends on the development of rice varieties adapted to specific edaphoclimatic and agroclimatic conditions, combined with appropriate cultural practices, including the use of fertilizers and integrated pest and disease management [2], as external factors such as climate and soil directly influence the development, yield, and grain quality of rice [11,12].

On the other hand, climate change and its associated effects such as prolonged droughts, intense rainfall, and increased prevalence of pests and diseases, have led to significant reductions in crop yields and productivity [13,14]. As a consequence, these factors create uncertainty for farmers, who growing challenges in adapting their agronomic practices to increasingly variable and unpredictable conditions [15]. In response to these challenges, various technologies have been implemented and adopted in recent years to optimize resource use and improve yields [16]; among these technologies, remote sensing has emerged as a promising tool because of its capacity to monitor agroclimatic variables in real-time and across multiple spatial scales [17,18], Remotely piloted aircraft systems (RPASs) provide data at significantly higher spatial resolution than satellites do [17], and although both technologies can be used to assess crop health status [17,19,20] and to predict agronomically important variables [21,22], RPAS-derived data generally allow for greater precision in estimations [17].

The potential of data mining in modeling the complex patterns in diverse research domains [23], is a notable consideration. Machine learning models, including nonlinear or autoregressive neural network (NAR-NNs) [24,25] and Gaussian process regression [26,27], allow the prediction of commodity price changes. Among the most relevant agronomic variables, crop yield stands out because of its direct impact on decision-making in crop management, particularly when timely information is available [20]. At a larger scale, early yield estimation enables the assessment of the productive capacity of a plot before harvest [28], the identification of low-yielding areas, and the optimization of fertilizer application—contributing to cost reduction and decreased environmental impacts [22,28]. In addition, accurate yield prediction aids the logistical planning of harvesting, storage, and marketing processes, facilitating negotiations with buyers [21]. In rice cultivation, yield has been effectively estimated through the modeling of RPAS-derived imagery combined with field data such as plant height [10,29–32]. The most commonly used modeling algorithms include artificial neural networks, linear regression models, random forests regression and support vector machines, all of which have demonstrated efficiency in predicting crop yields [10,33].

In summary, sensors integrated into RPAS platforms enable highly accurate monitoring of crop development throughout their phenological stages [34,35]; the integration of mathematical modeling techniques facilitates the estimation of phenological metrics [15,36,37], the mapping of responses to external factors such as diseases or water stress [20,38]; and the estimation of foliar indices [39] and agronomic variables such as nitrogen concentration, total biomass [10] and yield [21,29,40–42]. While this represents a significant advancement in modern agriculture, leading to higher production yields, maintaining or reducing production costs, and optimizing agronomic, economic, and environmental efficiency through the proper application of agricultural inputs [33,43], there remains a need to evaluate its effectiveness and performance across different environments and crop varieties [21]; furthermore, it is essential to explore alternatives on the basis of field-derived data to improve the fit of models [44]. Notably, in many

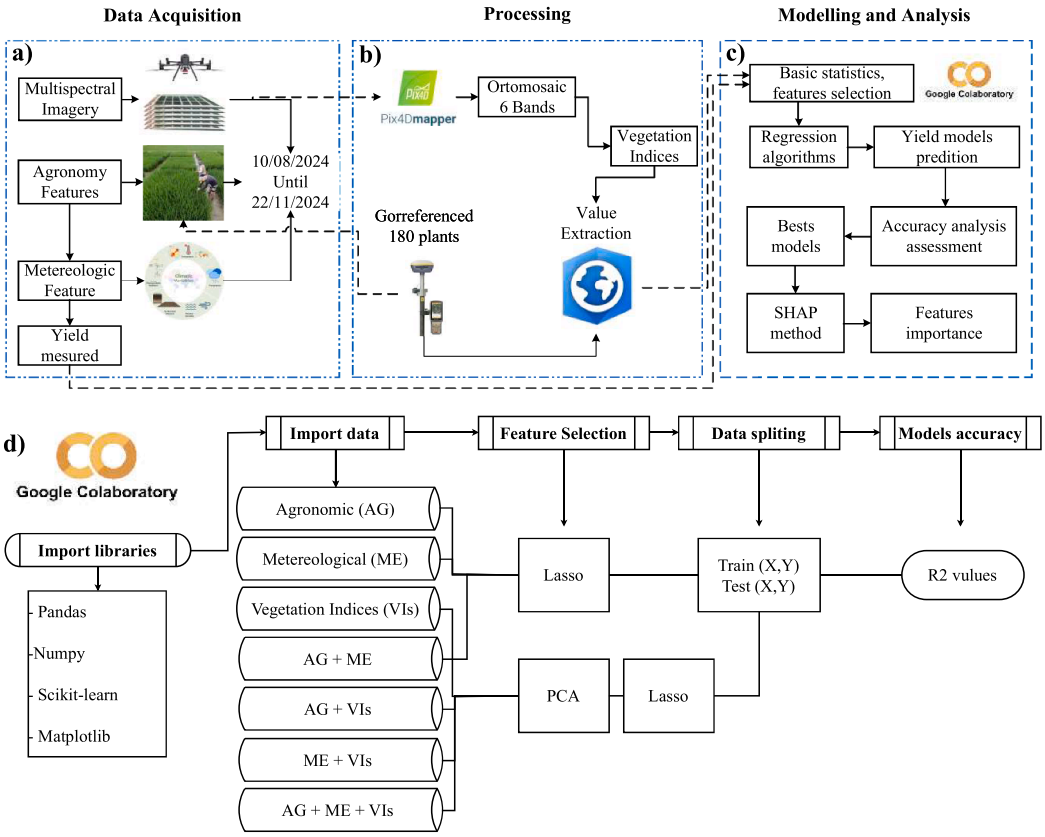

Fig. 2. General methodological framework applied to rice yield prediction. a) Data acquisition, which encompasses the collection of spectral, agronomic, meteorological, and yield information; b) processing, involving the computation of vegetation indices (VIs) per experimental unit; c) modeling and analysis, which includes the implementation of regression algorithms, model evaluation, and identification of key predictive variables; and d) implementation of regression algorithms conducted in the Google Colaboratory environment.

cases, the available models exhibit limited explanatory power owing to the "black box" nature of the data mining algorithms they employ [45].

In this context, the integration of agronomic data, vegetation indices (VIs), and meteorological information constitutes a robust approach for monitoring phenological development and estimating rice yield. Unlike previous studies, this study includes field variables in addition to VIs, and feature selection techniques are used to identify key variables that contribute to improving yield prediction accuracy. The Shapley Additive exPlanations (SHAP) method is also implemented to assess the individual contribution of each variable to model performance, thereby enhancing the interpretability of the results.

2. Materials and methods

2.1. Study area

This study was conducted at the Yanayacu Experimental Center, which is located in the district and province of Jaén, Cajamarca region, Peru. This experimental center is part of the Estación Experimental Baños del Inca which belongs to the Instituto Nacional de Innovación Agraria (INIA). The study area is characterized by a climate with temperatures ranging from 19 °C to 33 °C and an average annual rainfall between 350 mm and 1000 mm [46], as well as soils classified as eutric Regosols and haplic Calcisols.

The experiment was carried out using a randomized complete block design (RCBD). Six rice varieties (Victoria, Esperanza, Bellavista, Puntilla, Capoteña, and Valor) were evaluated, referred to as treatments. These were distributed across three blocks, with experimental units measuring 4 m × 3 m, resulting in a total of 18 experimental units. All the plots were managed under uniform irrigation and fertilization conditions. The varieties were sown in seedbeds on August 10, 2024. Fertilization was applied in four stages, with a total of 282 kg/ha of nitrogen (N), 115 kg/ha of phosphorus (P), and 52 kg/ha of potassium (K). Harvesting was carried out on November 22 of the same year (Fig. 1).

2.2. Methodological flow

The methodological design of this research is based on an integrated multivariate approach that systematically articulates four key components: (1) agronomic variables, (2) historical meteorological data, (3) VIs derived from remote sensors, and (4) machine learning algorithms developed specifically for rice yield prediction. This comprehensive methodological framework is illustrated in Fig. 2a–d, which outlines the data processing workflow from acquisition to the generation of predictive models.

2.3. Monitoring the phenological stages of rice using agronomic variables

The rice varieties were evaluated across six phenological stages 11, 30, 48, 68, 86, and 104 days after sowing (DAS) in the final field plot (Fig. 3). The collection of agronomic data began with the georeferencing of 180 plants, which were evenly distributed across 18 experimental units corresponding to six rice varieties, with three replicates each (Fig. 1). The plants were subsequently labeled with unique identification codes to facilitate measurements and ensure consistent tracking throughout the study period. The in-situ measurements included plant height (pH), number of tillers (NT), and chlorophyll content (CL), the latter of which was measured using a portable SPAD 502 chlorophyll meter – (Japan).

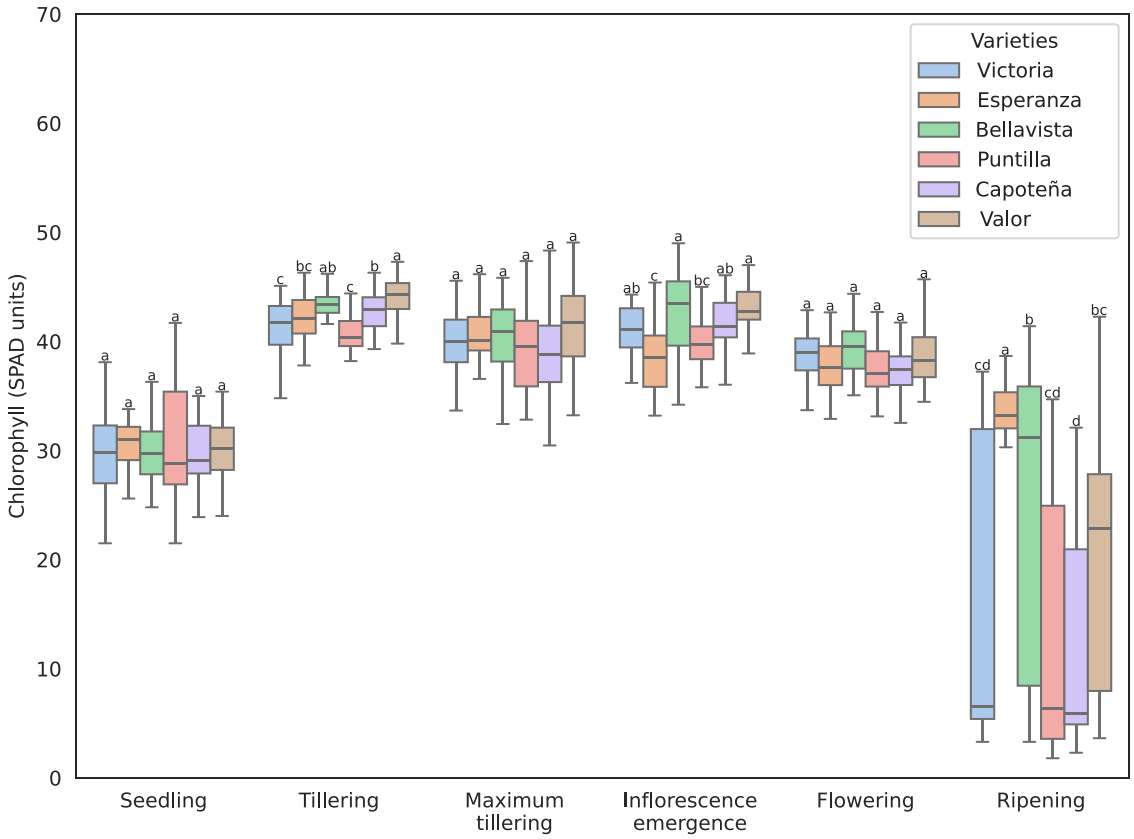

Fig. 3. Evaluation time points according to phase, phenological stage, and days after sowing (DAS).

The collected data were then utilized to generate boxplots, which were employed to visualize the temporal evolution. A One-way analysis of variance (ANOVA) was used to determine statistically significant differences, followed by Tukey's multiple comparison test ($p \leq 0.05$) to identify groups of rice varieties that exhibited significantly different characteristics. Statistical analyses and data visualization were performed in Google Colaboratory using the following Python packages: pandas, matplotlib, seaborn, scipy.stats, and statsmodels.

2.3.1. *Monitoring the phenological stages of rice using VIs*

Multispectral images were acquired using a DJI Matrice 350 RTK RPAS – (China) equipped with a Micasense RedEdge-P sensor (six bands: 475 nm, 560 nm, 668 nm, 717 nm, 842 nm, and 634.5 nm) – (United States). Flights were conducted at an altitude of 15 m and a speed of 2 m/s, with 70 % lateral and 80 % frontal overlap. This resulted in photogrammetric products with an approximate spatial resolution of 1 cm/pixel. Data acquisition was performed under optimal atmospheric conditions, between 10:00 and 14:00 h.

The processing of multispectral data began with the generation of six-band orthomosaics using Pix4Dmapper 4.5, which is based on geospatial images captured during the RPAS flights. To ensure accurate georeferencing of the orthophotos, three ground control points (GCPs) were established in the field using a South Galaxy G7 GNSS receiver – (China). Subsequently, 20 VIs (Table 1) were calculated on the basis of the spectral reflectance values processed in ArcGIS Pro 3.4 (Fig. 2b). Buffers (0.20 m) were created around the georeferenced plant points, and the specific index values within each buffer were averaged to obtain a representative value per plant. After the VIs were calculated, a normalized difference vegetation index (NDVI) map was generated to graphically illustrate the changes in the index across the different phenological stages of the crop. A boxplot was then produced to display the formation of significantly different groups, as determined by Tukey's HSD test. In addition, VIs were classified according to the spectral bands they utilize and their intended purpose. The values were averaged and visualized using heatmaps.

2.3.2. *Monitoring the phenological stages of rice using meteorological data*

Meteorological data were recorded daily throughout the entire crop cycle, from sowing to harvest, using a weather station from the National Service of Meteorology and Hydrology of Peru (SENAMHI), which is located 160 m from the experimental plot. The evaluated parameters are displayed as line charts; for their inclusion as independent variables in yield estimation models, temperature and relative humidity were averaged, while precipitation was recorded as cumulative [63]. Additionally, wind speed data were collected; however, this parameter was not included in the yield prediction models because of its low correlation with response variables, such as Temp = temperature (°C), RH = relative humidity (%) and P = precipitation (mm). The three variables of interest were measured using the same collection method, which is known as indirect measurement.

2.3.3. *Measurement of yield in rice varieties*

On day 104 after sowing, 180 evaluated plants were harvested, and individual plant yield values were obtained. These values were employed as inputs in regression algorithms to develop yield estimation models. Additionally, all 18 experimental units were harvested to project yield per hectare and the average yield per variety was calculated. To determine significant differences in yield among the six rice varieties, a normality test was conducted using the Shapiro–Wilk test, and homogeneity of variance was assessed with Levene's test. Once these assumptions were met, an analysis of variance (ANOVA) was performed using the Google Collaboratory platform.

2.3.4. *Yield estimation*

Crop yield was estimated using agronomic information, VIs, and meteorological data as input variables. To explore which combinations

Table 1
List of vegetation indices (VIs) calculated in this study, including their formulas and respective references. The indices were derived from spectral bands: red (R), green (G), blue (B), red edge (RE) and near-infrared band (NIR) bands.

N°	Indices	Formula	Reference
1	Normalized difference vegetation index	$NDVI = \frac{NIR - R}{NIR + R}$	[47]
2	Difference vegetation index	$DVI = NIR - R$	[47]
3	Ratio vegetation index	$RVI = \frac{NIR}{R}$	[48]
4	Transformed NDVI	$TNDVI = \sqrt{\frac{NIR - R}{NIR + R} + 0.5}$	[49]
5	Renormalized DVI	$RDVI = \frac{NIR - R}{\sqrt{(NIR + R}}$	[50]
6	Modified simple ratio	$mSR = \frac{\frac{NIR}{R} - 1}{\sqrt{\left(\frac{NIR}{R} + 1\right)}}$	[51]
7	Soil adjusted vegetation index	$SAVI = \frac{(NIR - R)(1 + 0.5)}{NIR + R + 0.5}$	[47]
8	Optimized SAVI	$OSAVI = 1.16.\frac{NIR - R}{NIR + R + 0.16}$	[52]
9	Modified soil adjusted vegetation index	$MSAVI = 0.5.\left[2NIR + 1 - \sqrt{(2NIR + 1)^2 - 8(NIR - G)}\right]$	[53]
10	Enhanced vegetation index	$EVI = 2.5 * \frac{NIR - R}{(NIR + 6R - 7.5B) + 1}$	[48]
11	Green normalized difference vegetation index	$GNDVI = \frac{NIR - G}{NIR + G}$	[54]
12	Green DVI	$gDVI = NIR - G$	[51]
13	Normalized green index	$NGI = G/(R + G + B)$	[55]
14	Chlorophyll index green	$CIgreen = \left(\frac{NIR}{G}\right) - 1$	[56]
15	Chlorophyll index rededge	$Clre = (NIR/RE) - 1$	[57]
16	Leaf chlorophyll index	$LCI = \frac{NIR - RE}{NIR + R}$	[58]
17	Transformed chlorophyll absorption ratio index	$TCARI = 3.[(RE - R) - 0.2(RE - G)(RE/R)]$	[59]
18	Modified chlorophyll absorption in reflectance index 1	$MCARI = [(RE - R) - 0.2 * (RE - G)] * \frac{RE}{R}$	[60]
19	Chlorophyll vegetation index (CVI)	$CVI = \frac{(NIR * R)}{G^2}$	[61]
20	Structure insensitive pigment index	$SIPI = \frac{NIR - B}{NIR - R}$	[62]

of variables were most suitable for yield estimation, the following scenarios were considered: (1) agronomic, (2) meteorological, (3) VIs, (4) AG + ME, (5) AG + VIs, (6) ME + VIs, and (7) AG + ME + VIs. Combinations that included VIs underwent a principal component analysis (PCA) to identify the 12 most important features. The LASSO algorithm was subsequently applied to reduce the number of features, prevent overfitting, and improve model interpretability [34]. Finally, the following regression algorithms were implemented: linear regression (LR), polynomial regression (PR), support vector regression (SVR), decision tree regression (DTR), and random forest (RF), using Python scripts executed in Google Colaboratory (Fig. 2d).

Regression algorithms were applied in Google Colaboratory, primarily using the scikit-learn library [64] along with NumPy and Pandas. For linear regressions, the linear regression function was used [65]. To implement decision tree regression, the decision tree regressor function was imported from the sklearn.tree module, with a random state value of 0 and a maximum depth of 5 [66]. For random forest regression, the random forest regressor function was imported from the sklearn.ensemble module [67], which uses 100 trees (n_estimators = 100) and sets the random state to 0. Polynomial regression was constructed using the polynomial features function with a second-degree polynomial [68]. For support vector regression (SVR), the input data were first standardized using the standard scaler [44]. The SVR function was then imported from the sklearn.svm module, and the radial basis function (RBF) kernel was used as the kernel function for SVR [69,70].

To evaluate the regression models, the coefficient of determination (R^2) was calculated (Eq. (1)), via the implementation available in scikit-learn [71], and the models with the best fit were selected. In this context, $\hat{y}_i$ represents the predicted value of the i th sample, and y_i is its corresponding observed value in a dataset of n samples (Eq. (2)). The values of this goodness-of-fit metric range from $-\infty$ to 1, with 1 indicating a perfect fit, whereas negative values suggest that the model performs arbitrarily worse than a horizontal mean line does [72].

sssss (1)

sssss (2)

Finally, for the best-performing models by variety, the Shapley Additive exPlanations (SHAP) technique was implemented. SHAP allows for the interpretation of decisions made by data mining models and helps identify the key features contributing to their predictions [72].

3. Results

3.1. Agronomic variables

3.1.1. Plant height and number of tillers

The rice varieties presented significant differences ($p < 0.05$) from the seedling stage, with Valor exhibiting a significantly greater plant height (25–41.5 cm) than the other varieties did (Fig. 4a). During the tillering stage, Victoria, Capoteña, and Valor (38.3–69.5 cm) were significantly taller than the other varieties were. From the flowering stage onward, growth stabilized until the Ripening phase. In this final stage, Victoria (110–135 cm) was significantly taller than Bellavista (96–119 cm), Puntilla and Capoteña (92–110 cm), and Esperanza and Valor (79–108 cm) were (Fig. 4a). The Victoria and Bellavista were classified as intermediate in height, whereas Puntilla, Capoteña, Esperanza, and Valor were classified as semidwarf.

Among the six evaluated rice varieties, the average number of tillers during the seedling stage was five, with no significant differences observed at this stage ($p < 0.05$) (Fig. 4b). The number of tillers increased progressively until the maximum tillering stage, with Puntilla (+433 %) and Valor (+416 %) showing the greatest increases, whereas Bellavista (+355 %) and Victoria (+349 %) presented the least tillering development. After the maximum tillering stage, all the varieties presented evidence of tiller abortion. Victoria (−26.6 %) and Bellavista (−24.2 %) presented the higher abortion rates, than Valor (−7.1 %) and Puntilla (−14 %) did. During the inflorescence emergence stage, the number of tillers tended to stabilize, with reductions ranging from −7 % to −0.1 %. In the ripening stage, the varieties that recorded the greatest number of fertile tillers were Puntilla and Valor (9–28), which were significantly different from Esperanza (8–26), Victoria (8–25), and Bellavista and Capoteña (8–26) (Fig. 4b).

3.1.2. Chlorophyll

The SPAD values of the six rice varieties tended to increase from the seedling stage (13–43.3) to the maximum tillering stage (30.5–49.0) (Fig. 5). No significant differences were detected during the seedling, maximum tillering, and flowering stages ($p > 0.05$). During ripening stage, a generalized decrease in SPAD values was observed across all the varieties, with significant differences detected among them ($p < 0.05$). During this stage, the varieties with the highest chlorophyll content were Bellavista (3.3–41.4), Valor (3.6–42.3), and Esperanza (21.5–38.7), the latter exhibiting the lowest standard deviation (σ = 10.46) (Fig. 5).

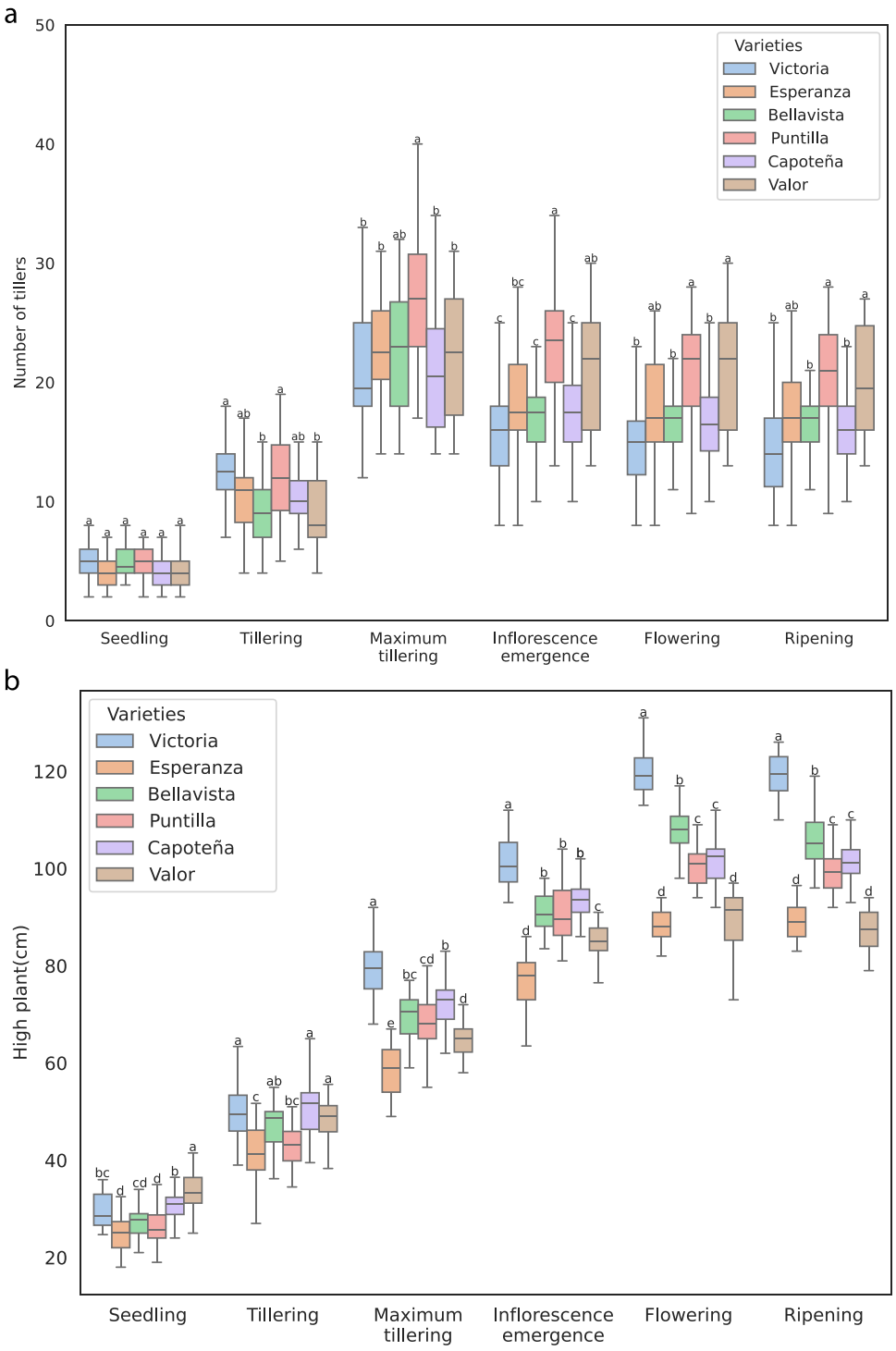

Fig. 4. Phenological development of six rice varieties assessed through a) plant height (cm) and b) number of tillers across six growth stages: seedling, tillering, maximum tillering, inflorescence emergence, flowering, and ripening. Each boxplot represents the median, interquartile range, and variability within each variety: Victoria (blue), Esperanza (orange), Bellavista (green), Puntilla (red), Capoteña (purple), and Valor (brown). The different letters above the boxes indicate statistically significant differences among varieties within each phenological stage ($p < 0.05$, Tukey's HSD test).

3.2. Vegetation indices

The NDVI map shows an upward trend in pixel values during the first four phenological stages, starting with an average of 0.32 in the seedling stage and reaching peak mean values of 0.93 and 0.95 during the maximum tillering (Fig. 6a–c) and inflorescence emergence stages (Fig. 6d), respectively. In the flowering and ripening stages, the greatest declines were observed, with the NDVI values even reaching negative levels (Fig. 6e and f).

The individually evaluated plants initially presented an increasing trend in the NDVI values, with a homogeneous pattern observed during the seedling and tillering stages (Fig. 7). From the maximum tillering stage onward, the varieties began to; significantly differ; the variance among them decreased from this stage through inflorescence emergence.; the variances subsequently increased, with all varieties showing statistically significant differences during the ripening stage (Fig. 7).

Phase	Vegetative			Reproductive		Ripening
Phenological stages	Seedling	Tillering	Maximum tillering	Inflorescence emergence	Flowering	Ripening
Days After Sowing (DAS)	11	30	48	68	86	104

Fig. 5. Chlorophyll content (SPAD units) of the six rice varieties across six phenological stages: seedling, tillering, maximum tillering, inflorescence emergence, flowering, and ripening. The boxplots display the median, interquartile range, and variability of chlorophyll values for each variety: Victoria (blue), Esperanza (orange), Bellavista (green), Puntilla (red), Capoteña (purple), and Valor (brown). The letters above the boxplots indicate statistically significant differences among varieties within each phenological stage ($p < 0.05$, Tukey's HSD test).

Analysis of the mean values of VIs across the phenological stages of the rice crop revealed a progressive increase from the seedling stage, with values reaching peak values during maximum tillering, inflorescence emergence, and flowering, followed by a decrease during the ripening stage (Fig. 8). This trend was consistent for the vegetation indices based on the NIR and red bands (NDVI, RDVI, DVI, TNDVI, mSR, and RVI) (Fig. 8a), as well as for the optimized soil-adjusted vegetation indices (EVI, OSAVI, SAVI, and MSAVI) (Fig. 8b), and the green band vegetation indices (GNDVI, GDVI, and NGI) (Fig. 8c). The pigment indices (Clgreen, CIre, LCI, MCARI and CVI) also followed this general trend (Fig. 8d). However, the SIPI and TCARI exhibited opposite or partially opposite behaviors compared with the other VIs bands (Fig. 8d). The SIPI was high during seedling (1.37 ± 0.12), decreased during tillering (1.03 ± 0.03), stabilized in maximum tillering (1.00 ± 0.00) stages, and inflorescence emergence (1.00 ± 0.00), and then increased again from flowering onward, reaching its highest values during ripening (1.30 ± 0.21). On the other hand, the TCARI showed a fluctuating pattern, with its lowest values (−0.04 and −0.01) occurring between maximum tillering and flowering (Fig. 8d).

Whit respect to the observed variability, the RVI index showed the greatest dispersion, with standard deviations of σ = 6.89 during flowering and σ = 4.94 during maximum tillering (Fig. 8a). In contrast, mSR showed less variability during flowering (σ = 0.68) and ripening (σ = 0.58) (Fig. 8a). Among the pigment indices, Clgreen presented the greatest variability in inflorescence emergence (σ = 1.82) and flowering (σ = 1.65); the CVI presented the greatest variability during Ripening (σ = 0.64) and Flowering (σ = 0.51); CIre, similar to Clgreen, presented the greatest dispersion in Inflorescence Emergence (σ = 0.57) and Flowering (σ = 0.46) (Fig. 8d). Excluding these indices, the largest overall standard deviations were recorded during the flowering (0.02–0.22) and ripening stages (0.06–0.21). The variability decreased in the maximum tillering (0.01–0.13), tillering (0.04–0.10), seedling (0.02–0.06), and inflorescence Emergence (0.01–0.05) stages (Fig. 8). This was followed by a decline, with precipitation decreasing to 10.7 mm during the ripening stage (Fig. 9b). The temperature remained stable throughout the period, with an average of 27.8 °C and minimal variation (Fig. 9a). The relative humidity, with an average of 43.8 %, exhibited a fluctuating pattern—high values were observed during the seedling stage, followed by a slight decrease in tillering, an increase up to the inflorescence emergence stage, and a decline during flowering and ripening (Fig. 9c). These patterns reflect the climatic fluctuations that influence the phenological development of the crop.

3.3. Yield evaluation

All experimental units were harvested, and the yield per hectare was projected. The Valor variety presented the highest average yield 13.70 t/ha, followed by Esperanza 13.41 t/ha and Puntilla 13.17 t/ha (Fig. 10). Although Valor had the highest average, Puntilla and Esperanza reached higher values in one of their replicates, with variances of 1.53 and 2.18, respectively, both greater than the 0.69 variance observed for Valor. The yield values for each replicate and variety were subjected to normality and homogeneity of variance tests. The Shapiro–Wilk test indicated that the residuals followed a normal distribution ($W = 0.9403$, $p = 0.5288$), whereas Levene's test confirmed that the variances were homogeneous among varieties ($p = 0.8837$). ANOVA revealed a significant effect of variety on yield ($F = 3.39$, $p = 0.0386$); however, Tukey's HSD post-hoc test did not detect any significant differences between specific pairs of varieties ($p > 0.05$ in all comparisons).

3.4. Estimation and modeling for yield prediction

The combinations of agronomic variables (AG) and agronomic plus meteorological variables (AG + ME) produced similar R^2 values, Victoria (0.38–0.71) (Fig. 11a) and Esperanza (0.51–0.69) (Fig. 11b) performed best, whereas lower values were obtained for Bellavista (0.02–0.70) (Fig. 11c), and weak performance was observed for the remaining varieties (0.00–0.45). The combination of agronomic variables and VIs (AG + VIs), as well as the combined agronomic variables, meteorological variables, and VIs (AG + ME + VIs), showed identical performance in all the cases, with the highest R^2 values recorded for the Bellavista variety (0.72–0.80) (Fig. 11d), and the lowest recorded for Capoteña (0.00–0.19) (Fig. 11e). R^2 values for models using only meteorological variables (MEs) were excluded because of negative values. Finally, the combination of only VIs showed good performance across most varieties, with particularly strong fits for Bellavista (0.81) and Victoria (0.70).

In terms of algorithm performance, linear regression (LR) and polynomial regression (PR) performed best for the Victoria, with R^2 values ranging from 0.41 to 0.70 and 0.00 to 0.71, respectively (Fig

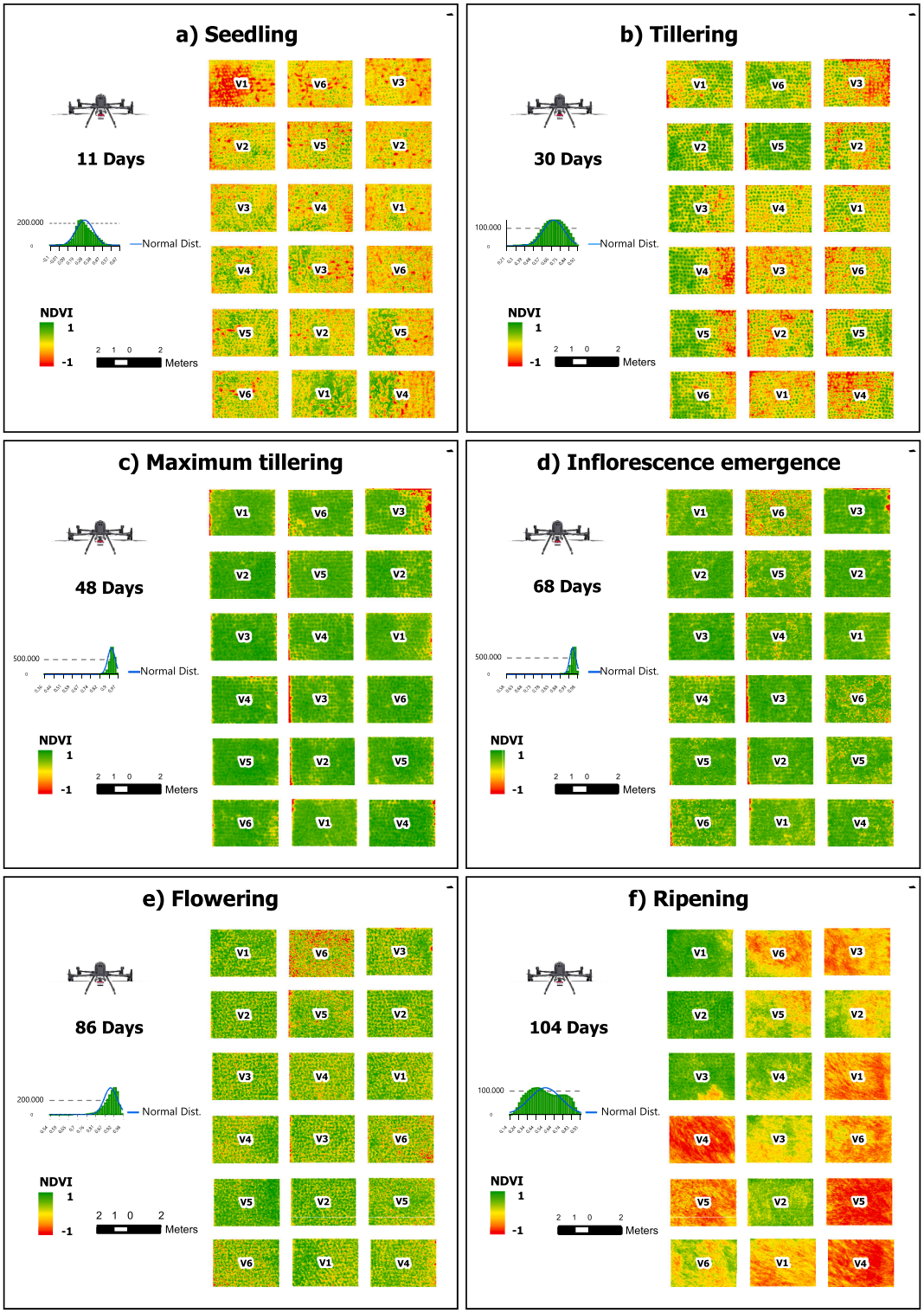

Fig. 6. Normalized difference vegetation index (NDVI) maps of six rice varieties (V1: Victoria, V2: Esperanza, V3: Bellavista, V4: Puntilla, V5: Capoteña, and V6: Valor) across six phenological stages: a) seedling (11 days), b) tillering (30 days), c) maximum tillering (48 days), d) inflorescence emergence (68 days), e) flowering (86 days), and f) ripening (104 days). The NDVI values are displayed using a standardized color scale ranging from –1 to 1, where higher values indicate greater vegetation vigor and greenness. Spatial distributions were derived from drone-based multispectral imagery and georeferenced to assess intravarietal differences in canopy development over time.

11a). For the remaining varieties, random forest regression (RFR) and decision tree regression (DTR) yielded the best fits, with maximum values of 0.80 for Bellavista (RFR) and 0.69 for Esperanza (DTR) (Fig. 11b). Finally, support vector regression (SVR) showed modest performance across most varieties but achieved the highest R^2 value recorded in the study for Bellavista (0.81) (Fig. 11c). For the Valor variety, SVR achieved a maximum R^2 of 0.61, with positive values in 4 out of the 6 variable combinations.

The maximum R^2 values by variety and phenological stage indicate that for Victoria, the tillering and flowering stages were the most

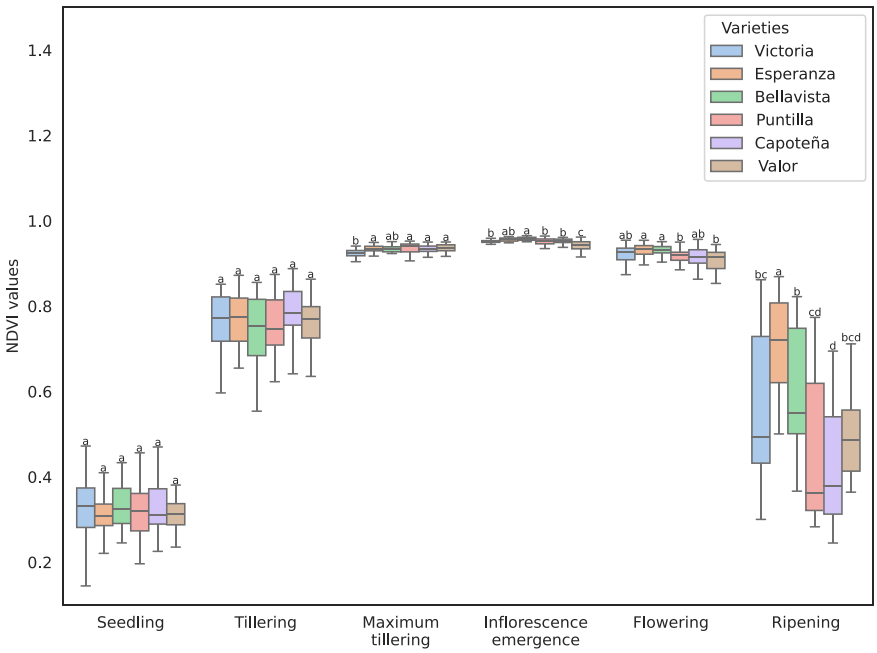

Fig. 7. Normalized difference vegetation index (NDVI) values of six rice varieties (Victoria, Esperanza, Bellavista, Puntilla, Capoteña, and Valor) across six phenological stages: seedling, tillering, maximum tillering, inflorescence emergence, flowering, and ripening. Each point represents the mean NDVI value for a given variety and stage. The vertical bars indicate standard deviations. The letters above the points denote statistically significant differences among varieties within each phenological stage ($p < 0.05$, Tukey's HSD test).

suitable for sampling, yielding R^2 values of 0.70 with linear regression (LR) and 0.71 with polynomial regression (PR). A similar pattern was observed for Esperanza, with R^2 values of 0.68 and 0.69. In contrast, for Bellavista, maximum tillering was the optimal stage, achieving the highest R^2 values with support vector regression (SVR) (0.81), random forest (RF) (0.80), and polynomial regression (PR) (0.60). Bellavista was also the variety with the two highest R^2 values recorded in the study (Fig. 12).

On the other hand, Puntilla, Valor, and Capoteña were the varieties with the lowest maximum R^2 values, reaching peaks of 0.67 and 0.61 during seedling, and 0.51 during tillering (Fig. 12). The most common optimal phenological stages for yield prediction were tillering (mode = 6), maximum tillering (mode = 6), and flowering (mode = 5). The varieties that presented the highest R^2 values were Bellavista (0.81) during the maximum tillering stage, and Victoria (0.71) and Esperanza (0.69) during the flowering stage (see Table 2). The models for Victoria and Esperanza were based on agronomic variables (AGs).

For the Victoria variety (Fig. 13a), the variable plant height was the most important, showing considerable dispersion in SHAP values, both positive and negative. Lower plant height values contributed the most to model accuracy, as did higher chlorophyll content and a lower number of tillers. On the other hand, for the Esperanza variety (Fig. 13b), the impact of the evaluated variables was less compared than that for Victoria, as reflected by the less dispersed and lower-magnitude SHAP values. In this variety, the most important variable was the number of tillers, indicating that greater numbers of tillers improved model accuracy, along with higher values of plant height and chlorophyll content.

4. Discussion

Crop monitoring is a key tool for agronomic management, as it enables the optimization of cultivation practices and supports evidence-based decision-making [73]. The integration of in situ monitoring, remote sensing techniques, and meteorological data allows for a more robust analysis of crop development [63], providing essential insights into crop growth and productive performance [18,63]. In this study, in situ observations, remote sensing techniques, and meteorological data were combined to assess the performance of six rice varieties throughout a full production cycle, offering detailed information on their phenological development, morphophysiological traits, and responses to specific environmental conditions.

During the monitoring of agronomic variables, differences among rice varieties were observed across phenological stages. The plant height followed an expected pattern, with accelerated growth occurring during the early stages and stabilization occurring during flowering and ripening (Fig. 4a). The heights of the varieties Esperanza, Bellavista, and Puntilla were within the expected range [74–76], while Capoteña, presented higher values [77], which was likely due to nitrogen overfertilization [78], as the applied dose slightly exceeded the recommended levels [79]. In addition to serving as an indicator of overfertilization [78], plant height is a particularly important trait especially in regions with high rainfall or strong winds, where the risk of lodging increases. In such environments, the cultivation of semidwarf varieties is more appropriate [80,81]. Therefore, Esperanza and Valor could represent promising alternatives for tropical areas with adverse climatic conditions, as well as opportunities for identifying genes associated with lodging resistance.

The number of tillers tended to increase from the seedling stage to maximum tillering stage and stabilized during the flowering stage (Fig. 4b), which is characteristic of rice development [82]. The Valor and Puntilla varieties presented the greatest number of fertile tillers (20.0 and 20.3 per plant, respectively). These values are less than those reported in India for the TKM 13 (26.9 per plant) and CO (R)50 (28.8 per plant) varieties, which are classified as medium-maturing, and CR 1009 Sub1 (36.2 per plant) and ADT 50 (34.4 per plant) varieties, which are late-maturing varieties [83]. The number of tillers is primarily a genetically determined trait; however, timely nitrogen fertilization also plays a critical role in its development [82,84]. Although tiller production is largely governed by genetic factors, fertilization significantly influences its expression [85]. Increasing nitrogen fertilizer doses can increase the number of tillers [86], which in turn leads to greater panicle production and higher crop yield [85] ultimately benefiting rice producers [87].

In terms of chlorophyll content, low values were observed during the

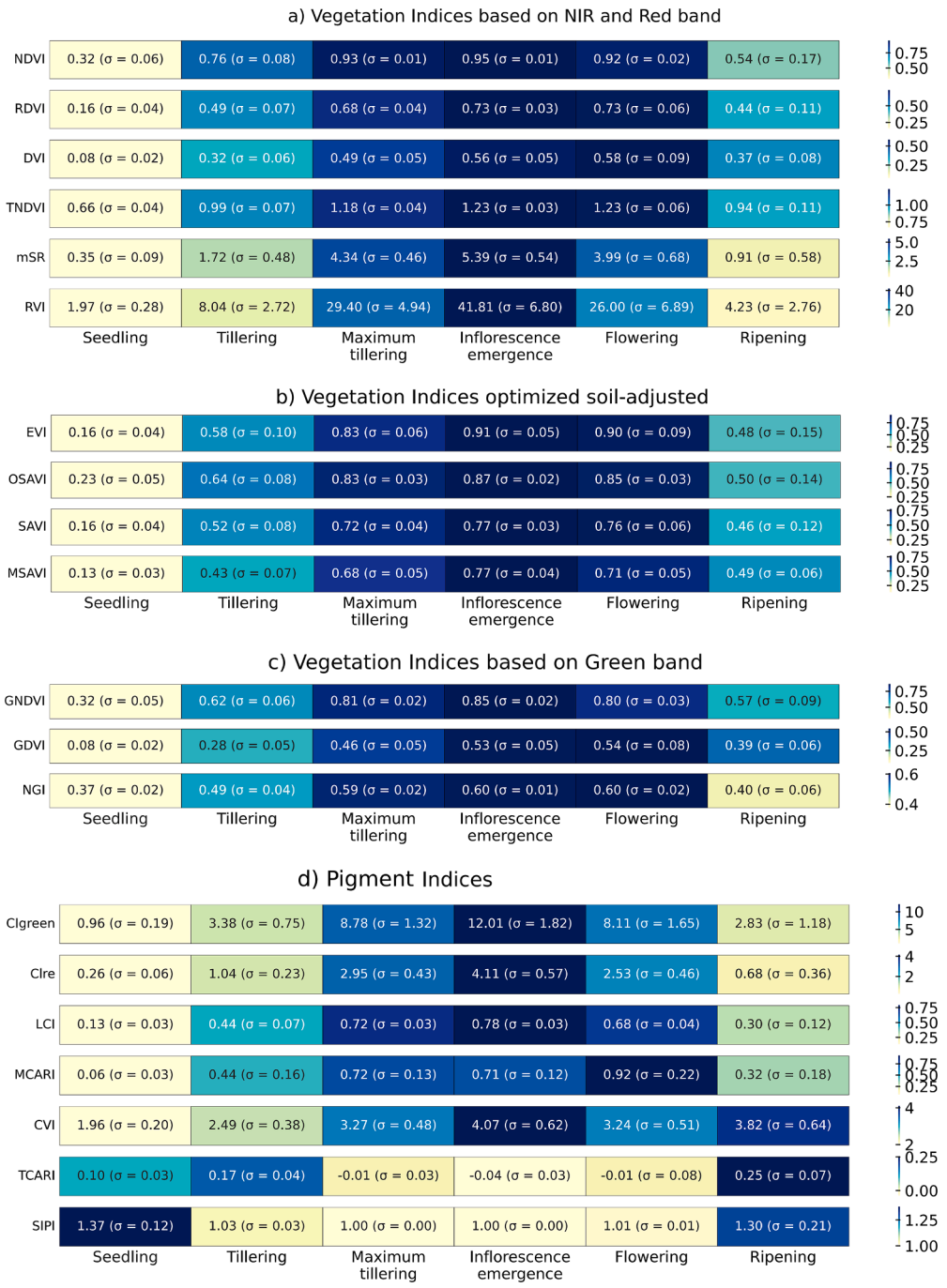

Fig. 8. Mean values and standard deviations of vegetation and pigment indices across six phenological stages of rice: seedling, tillering, maximum tillering, inflorescence emergence, flowering, and ripening. a) Indices based on NIR and red bands, b) soil-adjusted vegetation indices, c) indices based on the green band, and d) pigment-related indices. The heatmap color gradient represents the magnitude of each index, allowing visual comparison of spectral responses during crop development.

initial stages, followed by an increase during vegetative growth and a progressive decline during senescence (Fig. 5), in accordance with canopy development and photosynthetic activity [10,88]. The Esperanza, Bellavista, and Valor varieties maintained high chlorophyll levels even during the ripening stage, which may be attributed to their semi-early maturity characteristics [74,75,89]. These findings suggests that these varieties had not yet reached full physiological maturity at the time of evaluation [90]. In contrast, the Capoteña, Puntilla, and Victoria varieties [76,77], which are not necessarily classified as early maturing varieties, presented more abrupt and irregular declines in chlorophyll levels (Fig. 5). This behavior may represent a developmental disadvantage that could affect yield. Previous studies on the adaptation of genetically modified rice varieties support these findings [91], suggesting that chlorophyll dynamics are a key factor in the selection and management of cultivars with superior performance under varying agroclimatic conditions [90,91].

In relation to the monitoring of phenological stages using VIs, the NDVI is widely used because of its sensitivity to green biomass [92]. NDVI maps allow for the spatial and temporal visualization of crop physiological status [34]. In this study, the NDVI exhibited a unimodal growth pattern, with low values during the seedling stage (0.32) that increase until maximum values are reached during inflorescence

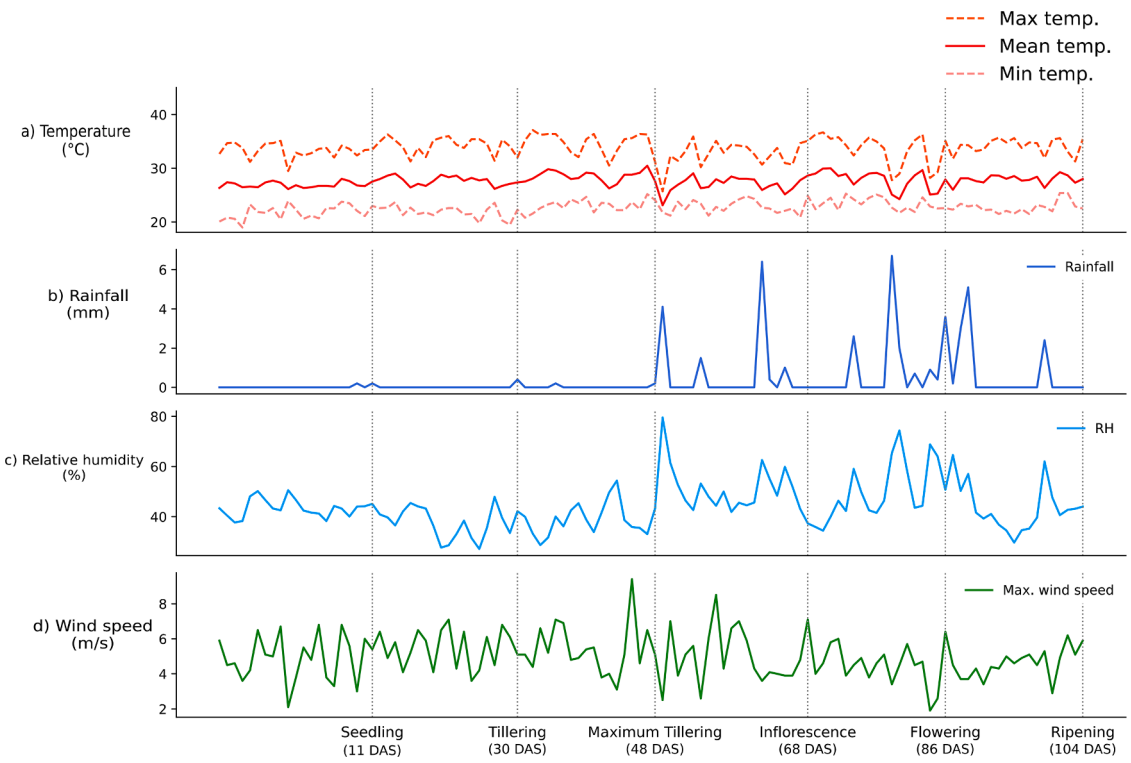

Fig. 9. Daily weather conditions recorded during the rice crop cycle, covering six phenological stages: seedling (11 DAS), tillering (30 DAS), maximum tillering (48 DAS), inflorescence emergence (68 DAS), flowering (86 DAS), and ripening (104 DAS). a) Temperature trends showing daily maximum, mean, and minimum values (°C); b) daily rainfall (mm); c) relative humidity (%); and d) maximum wind speed (m/s). These variables characterize the microclimatic dynamics influencing crop development throughout the growing season.

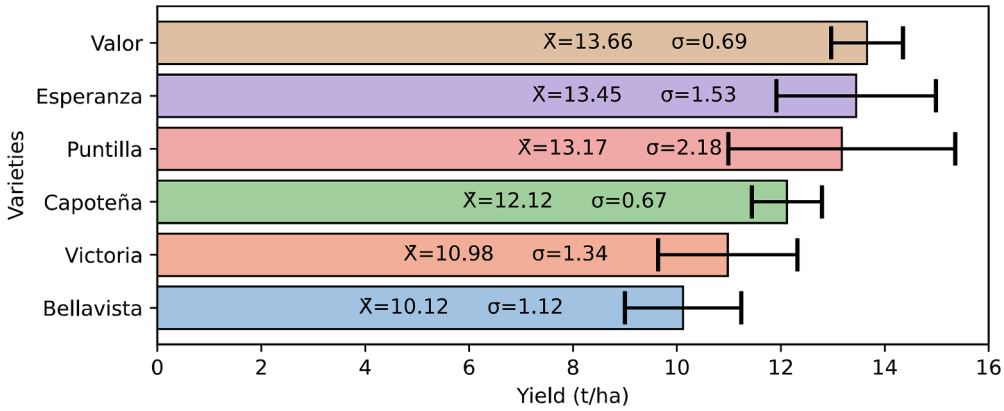

Fig. 10. Projected yield per hectare for the Valor, Esperanza, Puntilla, Capoteña, Victoria, and Bellavista rice varieties. $\bar{X}$ represents the mean yield, whereas σ denotes the standard deviation. Valor presented the highest projected yield (13.66 ± 0.69 t/ha), followed by Esperanza (13.45 ± 1.53 t/ha) and Puntilla (13.17 ± 2.18 t/ha). In contrast, Bellavista presented the lowest mean yield (10.12 ± 1.12 t/ha). The error bars indicate variability among replicates.

emergence (0.95) (Fig. 7), corresponding to increased leaf canopy coverage [38]. After the onset of flowering, the NDVI values began to decease, with the greatest difference observed during the ripening stage. These declines are associated with the beginning of the reproductive phase and the redistribution of resources toward grain filling [93]. By the ripening stage, clear differences were observed, particularly in the experimental units of Replication 3, which experienced lodging (Fig. 6). This issue was detected through NDVI mapping and has been previously reported, which complementing NDVI analyses using indices such as the NDRE, EVI, and MSAVI is recommended for more accurate assessments [35].

In addition to NDVI maps, VIs allow for real-time, nondestructive assessment of crop physiological status, serving as indicators of biomass, vigor, chlorophyll content, and stress levels [94]. VIs respond differently depending on the crop's phenological stage [36]. During the seedling stage, the NDVI (0.06) and GNDVI (0.05) (Fig. 8a and 8c) were greater than the other normalized indices. These indices tend to overestimate values under conditions of sparse vegetation [47,95]. In contrast, optimized soil-adjusted vegetation indices (Fig. 8b) produced lower values, more closely reflecting actual biomass content and proving useful for identifying plants that failed to establish properly due to sowing-related factors [47]. During the maximum tillering and inflorescence emergence stages, the NDVI values reached saturation, with the standard deviation decreasing to 0.01(Fig. 8a), which is a common limitation of this index [29,40,95]. Among the indices used, the EVI does not saturate with increased biomass [47], it shows greater standard deviation across

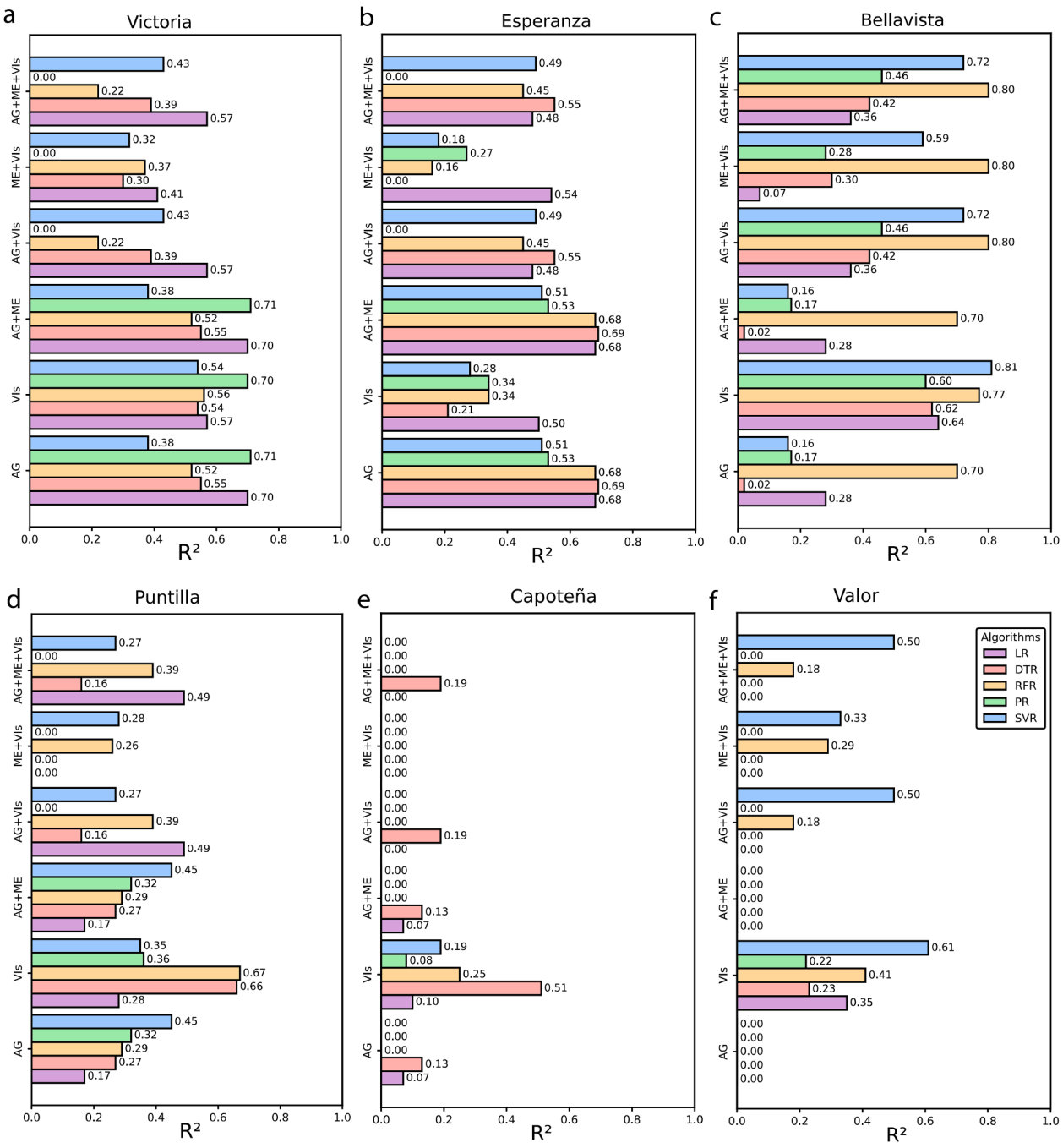

Fig. 11. Maximum coefficient of determination (R^2) values obtained from yield prediction models across six rice varieties: a) Victoria, b) Esperanza, c) Bellavista, d) Puntilla, e) Capoteña, and f) Valor. The models were constructed using five machine learning algorithms namely, linear regression (LR), decision tree regression (DTR), random forest regression (RFR), polynomial regression (PR), and support vector regression (SVR) and evaluated based on six different combinations of input features: agronomic data (AG), vegetation indices (VIs), agronomic + meteorological data (AG+ME), agronomic + vegetation indices (AG+VIs), meteorological + vegetation indices (ME+VIs), and Agronomic + Meteorological + Vegetation Indices (AG+ME+VIs). The bars represent the maximum R^2 values achieved for each feature set and algorithm combination per variety, highlighting the variability in model performance and feature importance across genotypes.

individual plants (Fig. 8b). This variability may be associated with significant differences in plant height (Fig. 4a) and chlorophyll content (Fig. 5) among varieties. The inflorescence emergence stage represents a critical point for nitrogen fertilization, as an adequate nitrogen supply ensures proper panicle formation and grain filling [93]. Although the NDVI values remained high during this stage, the GDVI was correlated with the chlorophyll content and was used to determine nitrogen requirements [96], with a standard deviation of 0.05 (Fig. 8c). This suggests that not all varieties or individual plants respond uniformly to nitrogen application [60], indicating the need for variety-specific fertilization strategies. This finding is further supported by the increase in the standard deviation to 0.08 during the flowering stage. Ripening is the final stage of the rice cycle, during which the crop completes grain filling, reaches physiological maturity, and progressively dries before harvest [97]. This stage presented the greatest degree of differentiation among the varieties and the highest standard deviation values (Fig. 8). During ripening, the NDVI values were negative in the NDVI map (Fig. 6f), which can indicate harvest readiness [37] or underlying physiological problems affecting crop health [35], both of which ultimately impact yield.

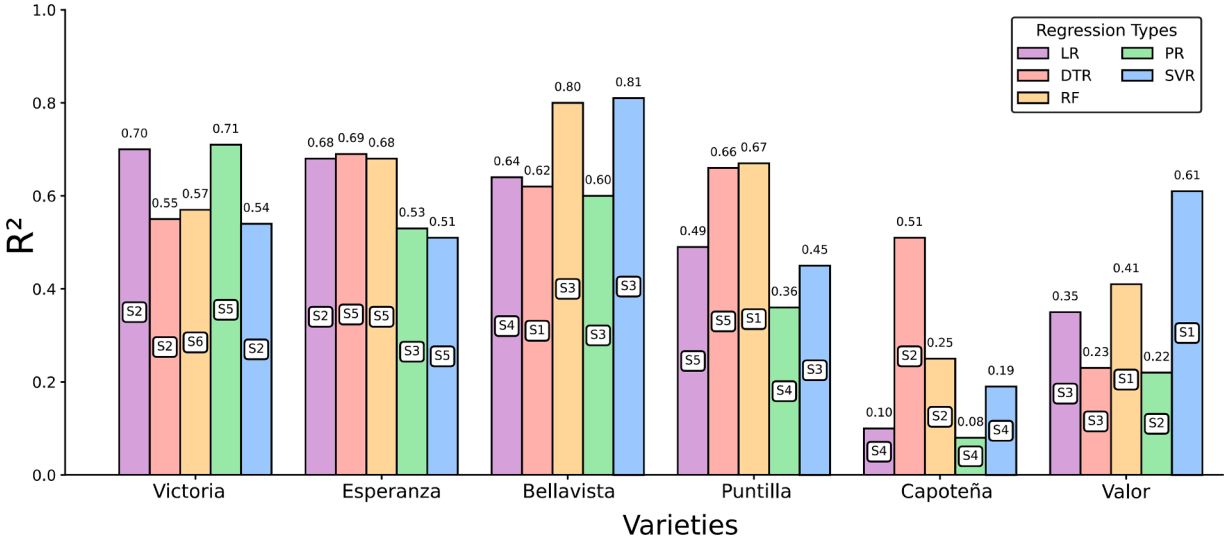

Fig. 12. Coefficient of determination (R^2) of the top-performing yield prediction models by rice variety and phenological stage using five regression algorithms: linear regression (LR), polynomial regression (PR), decision tree regression (DTR), random forest (RF), and support vector regression (SVR). The analysis spans six rice varieties (La Victoria, Esperanza, Bellavista, Puntilla, Capoteña, and Valor) and considers the best R^2 values achieved during specific phenological stages: S1 – seedling, S2 – tillering, S3 – maximum tillering, S4 – inflorescence emergence, S5 – flowering, and S6 – ripening. The labels within the bars indicate the phenological stage corresponding to each model's best performance.

Table 2
Summary of the best-performing yield prediction models for each rice variety, on the basis of the highest coefficient of determination (R^2). The table outlines the algorithm used, the phenological stage at which the best model performance was achieved, the type of input combination, and the specific variables that contributed most to model accuracy.

Variety	Algorithm	Stage	Combination	Inputs	R^2
Victoria	PR	Flowering	AG	High plant, tillers, chlorophyll	0.71
Esperanza	TD	Flowering	AG	High plant, tillers, chlorophyll	0.69
Bellavista	MSV	Maximum tillering	VIs	mSR	0.81
Puntilla	RF	Seedling	VIs	NDVI	0.67
Capoteña	TD	Tillering	VIs	GDVI	0.51
Valor	RF	Maximum tillering	VIs	RVI	0.61

The crop progressed from the seedling to maximum tillering stage during the dry season. During the vegetative growth phase, the average temperature did not exceed the critical threshold of 35 °C (Fig. 9a), which can inhibit shoot and root development as well as tiller proliferation [98]. The inflorescence emergence stage coincided with the onset of the rainy season; during this period, rainfall and relative humidity increased (Fig. 9b and 9c), helping to mitigate water stress a factor known to reduce the number of branches and spikelets, especially when temperatures exceed 33 °C, which can impair panicle development [99]; additionally, daytime temperatures above 35 °C or nighttime temperatures exceeding 32 °C are known to reduce pollen viability in rice [100]. During the flowering stage, one of the most climate-sensitive phases [101], the daytime temperatures did not exceed the sterility-inducing threshold of 37.2 °C [101], and the relative humidity remained close to 45 %, which is considered optimal. However, the occurrence of rainfall during flowering may have caused pollen washout or led to florets remaining closed [102], running the risk of prolonged rainy periods reducing light availability and increasing disease incidence, both of which can negatively affect grain settlement. During the ripening stage, environmental conditions influence the rate and duration of grain filling, as well as the final grain weight and quality [103]. The temperatures ranged between 20 and 35 °C (Fig. 9a), remaining close to the optimal range of 20–30 °C for grain filling [103]. However, the incidence of rainfall and strong winds caused lodging in the Puntilla and Capoteña varieties, a condition that tends to reduce yield [104]. Therefore, it is essential to select varieties that are suited to local environmental conditions and to develop crop calendars that align sowing periods with favorable weather windows, minimizing the risk of adverse climatic impacts during critical growth stages.

In terms of yield, the ANOVA test revealed significant differences among the rice varieties; however, Tukey's HSD post-hoc test was unable to clearly identify the best-performing varieties. This likely occurred because the significant differences were not sufficiently large [105]. In terms of the projected yields, the Valor (13.66 t/ha), Esperanza (13.45 t/ha), and Puntilla (13.17 t/ha) varieties presented the highest values (Fig. 10). Nevertheless, these yields are lower than those reported in some Asian regions, where production can reach 20 t/ha [106]. These differences may be attributed to genetic factors and differences in crop management practices [41]. While projected data are useful for extrapolating information from experimental trials, crop performance must be evaluated under real field conditions to obtain more representative and reliable results [107]. Therefore, research on larger-scale planting areas, which would allow for the generation of more accurate values that better reflect actual agronomic management practices, is recommended.

In terms of yield estimation, the performance of the variable combinations varied across the different rice varieties; however, Bellavista, Esperanza, and Victoria presented the best model fits (Fig. 11c, 11b and 11a). In general, combinations that included meteorological data were excluded because the LASSO algorithm implemented in the methodology disregards constant variables and selects only the most relevant features for the model [108]. Although other studies have used meteorological variables to increase model accuracy, these variables are typically included as nonconstant values, particularly at broader scales such as regional level analyses using satellite imagery [63]. Among the remaining combinations, the agronomic variables presented the best performance for the Victoria and Esperanza varieties, suggesting that this group of variables is more closely related to the yield of these specific genotypes. In contrast, for Bellavista, the VIs yielded the highest model performance, followed by the combination of VIs and agronomic

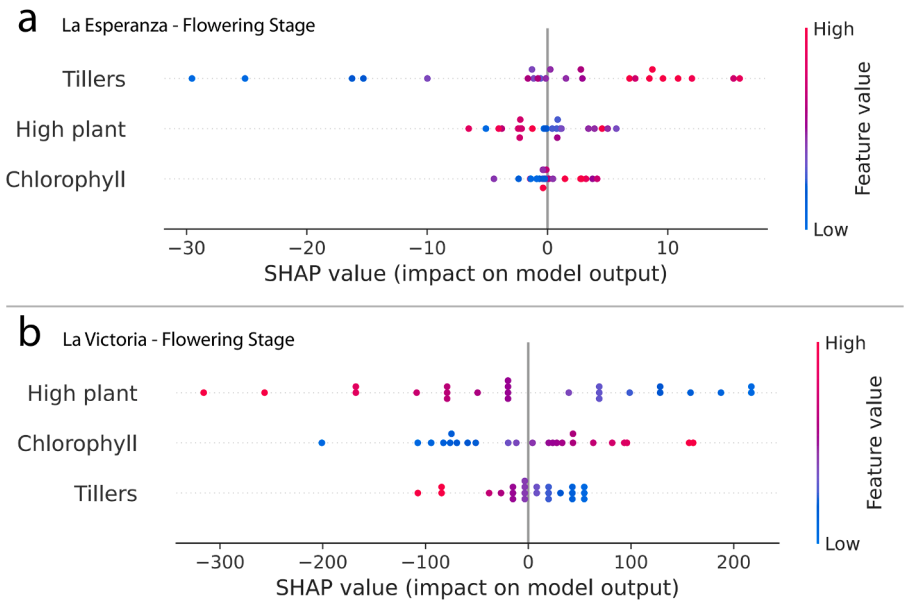

Fig. 13. SHAP summary plots showing the contributions of key agronomic variables to yield prediction models during the flowering stage for two rice varieties: a) Esperanza and b) Victoria. The x-axis represents the SHAP values, indicating the magnitude and direction of each feature's impact on the model's output. Each dot represents a single observation, colored according to the feature value (blue = low, pink = high).

variables. For the remaining varieties, the model fits were poor, which may be attributed to a weak correlation between the dependent variable (yield) and the predictor variables [109].

For Victoria and Esperanza varieties, the agronomic variables presented the best fit during the flowering stage (Fig. 12), likely because the plants tend to maintain their structural integrity up to the ripening stage, which is positively correlated with yield [10]. SHAP analysis revealed that the importance of predictive variables varies among varieties, indicating that plant height, number of tillers, and chlorophyll content are key factors to consider when developing yield prediction models (Fig. 13). In contrast, the Bellavista, Puntilla, Capoteña, and Valor varieties achieved better performance with VIs, particularly during early phenological stages from the seedling to maximum tillering stages (Fig. 12) likely because VIs do not reach saturation during these phases. This allows algorithms such as support vector regression, random forest, and decision tree algorithms to effectively utilize the available data to estimate yield. Our best-performing model used the mSR index values obtained during the maximum tillering stage, implemented through support vector regression. This finding is consistent with several studies [110] that also identified this phenological stage as optimal [10]. However, other authors have suggested Inflorescence Emergence as the most suitable stage for yield prediction [42], although the R^2 values reported in those cases (0.75) were lower than those obtained in this study (0.81). While our results are modest in a monotemporal evaluation approach, multitemporal studies have shown the potential to significantly improve model prediction accuracy, reaching R^2 values as high as 0.95 [29]; therefore, we recommend conducting studies with extended evaluation periods to collect more data and increase the predictive accuracy of yield estimation models.

The monitoring of agronomic variables, VIs, and meteorological conditions forms the basis for crop research, providing scientific evidence to support decision-making processes [73]. Although this study covered a full production cycle, making robust recommendations regarding the implementation of specific varieties requires evaluating their performance over at least three years and in different locations, as pest pressures, phenotypic responses, and yields may vary depending on seasonal conditions [107]. Additionally, the evaluation of a single fertilization rate limits the ability to determine optimal nutrient levels to maximize crop yield [78]. Nevertheless, the results obtained in this study provide a solid foundation for future research aimed at optimizing the management of high-performing rice varieties, thereby contributing to the development of more efficient and sustainable strategies for agricultural production.

5. Conclusions

This study evaluated six rice varieties throughout a complete production cycle, revealing distinct phenological responses under the specific environmental and agronomic conditions of the study area. Monitoring enabled the classification of varieties on the basis of plant height (the Victoria and Bellavista varieties exhibited intermediate heights, whereas the Puntilla, Capoteña, Esperanza, and Valor varieties were categorized as semidwarf), the identification of varieties with greater tillering capacity (Puntilla and Esperanza, with 9–28 tillers), and the recognition of the variety with the most stable chlorophyll content during the ripening stage (Esperanza, with SPAD values ranging from 21.5 to 38.7, and $\sigma = 10.46$). The use of vegetation indices (VIs) allowed for the detection of distinct spectral responses among varieties across developmental stages, with significant differences emerging particularly during ripening. Furthermore, the inclusion of meteorological variables contributed to explaining lodging events in the Capoteña and Puntilla varieties, which were associated with environments characterized by less precipitation. This monitoring approach underscores the importance to evaluate local varieties in a holistic manner to inform decision-making in rice cultivation. The integration of agronomic, spectral, and meteorological data demonstrated the potential of machine learning approaches for yield estimation, with support vector regression (SVR) exhibiting the highest predictive accuracy ($R^2 = 0.81$) for the Bellavista variety at the maximum tillering stage. The limitations of this work include the lack of historical field reports to standardize the application of inputs for each variety at the evaluation site. To increase the robustness and applicability of these methodologies, future research should consider broader spatial and temporal scales and further refine the use of VIs in relation to specific crop management practices.

Ethical statement

Instituto Nacional de Innovación Agraria

The present study did not involve human participants, animals, or the use of any personal or sensitive data. Therefore, ethical approval was not required. All experimental procedures were conducted in accordance with institutional, national, and international guidelines for responsible conduct of research. The authors confirm that the study complies with the ethical standards of the journal and relevant regulations.

CRediT authorship contribution statement

Jorge A. Fernandez-Jibaja: Writing – original draft, Visualization, Software, Methodology, Investigation, Formal analysis, Conceptualization. **Nilton Atalaya-Marin:** Writing – original draft, Visualization, Software, Methodology, Investigation, Conceptualization. **Yeltsin A. Álvarez-Robledo:** Visualization, Validation, Investigation, Data curation. **Victor H. Taboada-Mitma:** Supervision, Resources, Project administration, Funding acquisition. **Juancarlos Cruz-Luis:** Supervision, Resources, Project administration, Funding acquisition. **Daniel Tineo:** Writing – review & editing, Visualization, Supervision, Investigation, Conceptualization. **Malluri Goñas:** Writing – review & editing, Visualization, Supervision, Investigation, Conceptualization. **Darwin Gómez-Fernández:** Writing – review & editing, Visualization, Supervision, Methodology, Investigation, Conceptualization.

Declaration of competing interest

The authors declare that they have no known competing financial interests or personal relationships that could have appeared to influence the work reported in this paper.

Acknowledgments

This study was funded by Investment Project with CUI No 2472675: "Mejoramiento de los servicios de investigación y transferencia de tecnología agraria en la estación agraria experimental Baños del Inca en la localidad de Baños del Inca del distrito de Baños del Inca - provincia de Cajamarca - departamento de Cajamarca", Dirección de Servicios Estratégicos Agrarios (DSEA), Instituto Nacional de Innovación Agraria (INIA). The authors thank Teiser Sanchez, Pedro Torres, Larry García and Javier Yovera for their help in data collection.

Data availability

Data will be made available on request.

References

[1] FAO, Crops and livestock products, (2023). https://www.fao.org/faostat/es/#data/QCL/visualize (accessed January 15, 2025).
[2] M. Alam, G. Lou, W. Abbas, R. Osti, A. Ahmad, S. Bista, J.K. Ahiakpa, Y. He, Improving rice grain quality through ecotype breeding for enhancing food and nutritional security in Asia–Pacific Region, Rice 17 (2024), https://doi.org/10.1186/s12284-024-00725-9.
[3] MIDAGRI, Observatorio de Commodities Arroz - Enero/Marzo 2022, (2022). https://www.gob.pe/institucion/midagri/informes-publicaciones/3251275-commodities-trimestral-2022.
[4] FAO, Seguridad Alimentaria y Comercio Agroalimentario En América Latina y Caribe, Intl Food Policy Res Inst, Santiago, 2020.
[5] MIDAGRI, Observatorio de Commodities Arroz - Octubre/Diciembre 2022. https://www.gob.pe/institucion/midagri/informes-publicaciones/3251275-commodities-trimestral-2022, 2022 (accessed January 11, 2025).
[6] United Nations, World Population Prospects - Population Division, United Nations, 2019. https://population.un.org/wpp/.
[7] M. van Dijk, T. Morley, M.L. Rau, Y. Saghai, A meta-analysis of projected global food demand and population at risk of hunger for the period 2010–2050, Nat Food 2 (2021) 494–501, https://doi.org/10.1038/s43016-021-00322-9.
[8] FAO, Panorama de seguridad alimentaria y nutricional en América latina y Caribe, 2023. http://190.96.97.141:8889/xmlui/handle/123456789/178.
[9] J. Phillips, A. Durand-Morat, L.L. Nalley, E. Graterol, M. Bonatti, K. de Pava, S. Urioste, W. Yang, Understanding demand for broken rice and its potential food security implications in Colombia, J. Agric. Food Res. 15 (2024), https://doi.org/10.1016/j.jafr.2023.100884.
[10] D. Stavrakoudis, D. Katsantonis, K. Kadoglidou, A. Kalaitzidis, I.Z. Gitas, Estimating rice agronomic traits using drone-collected multispectral imagery, Remote Sens (Basel) 11 (2019) 545, https://doi.org/10.3390/rs11050545.
[11] N.K. Fageria, V.C. Baligar, Lowland rice response to nitrogen fertilization, Commun. Soil Sci. Plant Anal. 32 (2001) 1405–1429, https://doi.org/10.1081/CSS-100104202.
[12] D. Abebe, W. Mohammed, A. Tesfaye, Genotype X environment interaction and stability analysis in upland rice (Oryza sativa L.) varieties in Ethiopia, J. Crop Sci. Biotechnol. 26 (2023) 51–62, https://doi.org/10.1007/s12892-022-00161-5.
[13] C.A. Deutsch, J.J. Tewksbury, M. Tigchelaar, D.S. Battisti, S.C. Merrill, R.B. Huey, R.L. Naylor, Increase in crop losses to insect pests in a warming climate, Science (1979) 361 (2018) 916–919, https://doi.org/10.1126/science.aat3466.
[14] R. Hidayat, Climate change impacts, adaptation and mitigation in the agricultural sector, Global J. Environ. Sci. Manag. 10 (2024) 1457–1476, https://doi.org/10.22034/gjesm.2024.03.30.
[15] D. Wasif, M.Q. Khan, R. Murtaza, M.Z. Ahmad, Z. Zafar, M. Shahzad, K. Berns, M. M. Fraz, Extraction of Rice phenological metrics using temporally correlated multispectral drone imagery, IEEE (2022) 163–169, https://doi.org/10.1109/SITIS57111.2022.00039.
[16] Z. Ramli, A.S. Juraimi, M. Motmainna, N.N. Che'ya, M.H.M. Roslim, N.M. Noor, A. Ahmad, Weed management using UAV and remote sensing in Malaysia Paddy field: a review, Pertanika J. Sci. Technol. 32 (2024) 1219–1241, https://doi.org/10.47836/PJST.32.3.13.
[17] S.A. Gade, M.J. Madolli, P. García-Caparrós, H. Ullah, S. Cha-um, A. Datta, S. K. Himanshu, Advancements in UAV remote sensing for agricultural yield estimation: a systematic comprehensive review of platforms, sensors, and data analytics, Remote Sens. Appl. 37 (2025) 101418, https://doi.org/10.1016/J.RSASE.2024.101418.
[18] A. Rejeb, A. Abdollahi, K. Rejeb, H. Treiblmaier, Drones in agriculture: a review and bibliometric analysis, Comput. Electron. Agric. 198 (2022), https://doi.org/10.1016/j.compag.2022.107017.
[19] Z. Gong, W. Ge, J. Guo, J. Liu, Satellite remote sensing of vegetation phenology: progress, challenges, and opportunities, ISPRS J. Photogramm. Remote Sens. 217 (2024) 149–164, https://doi.org/10.1016/j.isprsjprs.2024.08.011.
[20] M. Son Le, Y.-A. Liou, M.T. Pham, Crop response to disease and water scarcity quantified by normalized difference latent heat index, IEEE Access 11 (2023) 55938–55946, https://doi.org/10.1109/ACCESS.2023.3283033.
[21] B. Duan, S. Fang, Y. Gong, Y. Peng, X. Wu, R. Zhu, Remote estimation of grain yield based on UAV data in different rice cultivars under contrasting climatic zone, Field Crops. Res. 267 (2021), https://doi.org/10.1016/j.fcr.2021.108148.
[22] S. Pazhanivelan, R. Kumaraperumal, P. Shanmugapriya, N.S. Sudarmanian, A. P. Sivamurugan, S. Satheesh, Quantification of biophysical parameters and economic yield in cotton and rice using drone technology, Agric. (Switzerland) 13 (2023), https://doi.org/10.3390/agriculture13091668.
[23] X. Xu, Corn cash price forecasting, Am. J. Agric. Econ. 102 (2020) 1297–1320, https://doi.org/10.1016/j.compag.2021.106120.
[24] B. Jin, X. Xu, Y. Zhang, Peanut oil price change forecasts through the neural network, Foresight 27 (2025) 595–612, https://doi.org/10.1108/FS-01-2023-0016.
[25] B. Jin, X. Xu, China commodity price index (CCPI) forecasting via the neural network, Int. J. Financ. Eng. (2025) 1–27, https://doi.org/10.1142/S2424786325500033.
[26] B. Jin, X. Xu, Machine learning coffee price predictions, J. Uncertain Syst. 17 (2024), https://doi.org/10.1142/S1752890924500235.
[27] B. Jin, X. Xu, Predicting wholesale edible oil prices through gaussian process regressions tuned with bayesian optimization and cross-validation, Asian J. Econ. Banking 9 (2024) 64–82, https://doi.org/10.1108/AJEB-06-2024-0070.
[28] F.C. Eugenio, M. Grohs, M.S. Schuh, L.P. Venancio, C. Schons, T.L. Badin, C. L. Mallmann, P. Fernandes, S.D. da Silva, R.A. Fantinel, Flooded rice variables from high-resolution multispectral images and machine learning algorithms, Remote Sens. Appl. 31 (2023), https://doi.org/10.1016/j.rsase.2023.100998.
[29] N. Perros, D. Kalivas, R. Giovos, Spatial analysis of agronomic data and uav imagery for rice yield estimation, Agric. (Switzerland) 11 (2021), https://doi.org/10.3390/agriculture11090809.
[30] J. Enciso, C.A. Avila, J. Jung, S. Elsayed-Farag, A. Chang, J. Yeom, J. Landivar, M. Maeda, J.C. Chavez, Validation of agronomic UAV and field measurements for tomato varieties, Comput. Electron. Agric. 158 (2019) 278–283, https://doi.org/10.1016/j.compag.2019.02.011.
[31] D. Bhusal, D.P. Thakur, Precision nitrogen management on crop production: a review, Archiv. Agric. Environ. Sci. 7 (2022) 267–271, https://doi.org/10.26832/24566632.2022.0702016.
[32] B. Schauberger, J. Jägermeyr, C. Gornott, A systematic review of local to regional yield forecasting approaches and frequently used data resources, Eur. J. Agron. 120 (2020) 126153, https://doi.org/10.1016/J.EJA.2020.126153.
[33] T. van Klompenburg, A. Kassahun, C. Catal, Crop yield prediction using machine learning: a systematic literature review, Comput. Electron. Agric. 177 (2020), https://doi.org/10.1016/j.compag.2020.105709.
[34] S. Samsuddin Sah, K.N. Abdul Maulud, S. Sharil, O.A. Karim, B. Pradhan, Monitoring of three stages of paddy growth using multispectral vegetation index derived from UAV images, Egyptian J. Remote Sens. Space Sci. 26 (2023) 989–998, https://doi.org/10.1016/J.EJRS.2023.11.005.
[35] Q. Yang, L. Shi, J. Han, Z. Chen, J. Yu, A VI-based phenology adaptation approach for rice crop monitoring using UAV multispectral images, Field. Crops. Res. 277 (2022), https://doi.org/10.1016/J.FCR.2021.108419.
[36] J. Zhang, X. Lin, C. Jiang, X. Hu, B. Liu, L. Liu, L. Xiao, Y. Zhu, W. Cao, L. Tang, Predicting rice phenology across China by integrating crop phenology model and

machine learning, Sci. Total Environ. 951 (2024), https://doi.org/10.1016/j.scitotenv.2024.175585.
[37] H. Ge, F. Ma, Z. Li, Z. Tan, C. Du, Improved accuracy of phenological detection in rice breeding by using ensemble models of machine learning based on uav-rgb imagery, Remote Sens (Basel) 13 (2021), https://doi.org/10.3390/rs13142678.
[38] S.K. Vishwakarma, B. Bhattarai, K. Kothari, A. Pandey, Mapping crop water productivity of rice across diverse irrigation and fertilizer rates using field experiment and UAV-based multispectral data, Remote Sens. Appl. 37 (2025), https://doi.org/10.1016/J.RSASE.2025.101456.
[39] W. Yuan, Y. Meng, Y. Li, Z. Ji, Q. Kong, R. Gao, Z. Su, Research on rice leaf area index estimation based on fusion of texture and spectral information, Comput. Electron. Agric. 211 (2023), https://doi.org/10.1016/j.compag.2023.108016.
[40] Z. Longfei, M. Ran, Y. Xing, L. Yigui, H. Zehua, L. Zhengang, X. Binyuan, Y. Guodong, P. Shaobing, X. Le, Improved yield prediction of ratoon rice using unmanned aerial vehicle-based multi-temporal feature method, Rice Sci. 30 (2023) 247–256, https://doi.org/10.1016/j.rsci.2023.03.008.
[41] D. Goigochea Pinchi, M. Justino Pinedo, S.S. Vega Herrera, M. Sanchez Ojanasta, R.H. Lobato Galvez, M.D. Santillan Gonzales, J.J. Ganoza Roncal, Z.L. Ore Aquino, A.I. Agurto Piñarreta, yield prediction models for rice varieties using UAV multispectral imagery in the Amazon lowlands of Peru, Agri Eng. 6 (2024) 2955–2969, https://doi.org/10.3390/AGRIENGINEERING6030170.
[42] G. Yang, Y. Li, S. Yuan, C. Zhou, H. Xiang, Z. Zhao, Q. Wei, Q. Chen, S. Peng, L. Xu, Enhancing direct-seeded rice yield prediction using UAV-derived features acquired during the reproductive phase, Precis Agric. 25 (2024) 1014–1037, https://doi.org/10.1007/s11119-023-10103-y.
[43] R. Casa, A. Cavalieri, B. lo Cascio, Nitrogen fertilisation management in precision agriculture: a preliminary application example on Maize, Italian J. Agron. 6 (2011) e5, https://doi.org/10.4081/IJA.2011.E5.
[44] W.H. Maes, K. Steppe, Perspectives for remote sensing with unmanned aerial vehicles in precision agriculture, Trends Plant Sci. 24 (2019) 152–164, https://doi.org/10.1016/j.tplants.2018.11.007.
[45] Y. Cai, K. Guan, D. Lobell, A.B. Potgieter, S. Wang, J. Peng, T. Xu, S. Asseng, Y. Zhang, L. You, B. Peng, Integrating satellite and climate data to predict wheat yield in Australia using machine learning approaches, Agric. For. Meteorol. 274 (2019) 144–159, https://doi.org/10.1016/J.AGRFORMET.2019.03.010.
[46] SENAMHI, Climas del Perú - Mapa de Clasifiación Climática Nacional, (2021). https://www.senamhi.gob.pe/?p=mapa-climatico-del-peru (accessed January 11, 2025).
[47] A. Bannari, D. Morin, F. Bonn, A.R. Huete, A review of vegetation indices, Remote Sens. Rev. 13 (1995) 95–120, https://doi.org/10.1080/02757259509532298.
[48] W.A. Dorigo, R. Zurita-Milla, A.J.W. de Wit, J. Brazile, R. Singh, M.E. Schaepman, A review on reflective remote sensing and data assimilation techniques for enhanced agroecosystem modeling, Int. J. Appl. Earth Obs. Geoinf. 9 (2007) 165–193, https://doi.org/10.1016/j.jag.2006.05.003.
[49] S. Goswami, S.S. Choudhary, C. Chatterjee, D.R. Mailapalli, A. Mishra, N. S. Raghuwanshi, Estimation of nitrogen status and yield of rice crop using unmanned aerial vehicle equipped with multispectral camera, J. Appl. Remote Sens. 15 (2021), https://doi.org/10.1117/1.JRS.15.042407.
[50] A.A. Gitelson, Wide dynamic range vegetation index for remote quantification of biophysical characteristics of vegetation, J. Plant Physiol. 161 (2004) 165–173, https://doi.org/10.1078/0176-1617-01176.
[51] C.J. Tucker, J.H. Elgin, J.E. McMurtrey, C.J. Fan, Monitoring corn and soybean crop development with hand-held radiometer spectral data, Remote Sens. Environ. 8 (1979) 237–248, https://doi.org/10.1016/0034-4257(79)90004-X.
[52] C.S.T. Daughtry, C.L. Walthall, M.S. Kim, E.B. de Colstoun, J.E. McMurtrey, Estimating corn leaf chlorophyll concentration from leaf and canopy reflectance, Remote Sens. Environ. 74 (2000) 229–239, https://doi.org/10.1016/S0034-4257(00)00113-9.
[53] D. Haboudane, J.R. Miller, E. Pattey, P.J. Zarco-Tejada, I.B. Strachan, Hyperspectral vegetation indices and novel algorithms for predicting green LAI of crop canopies: modeling and validation in the context of precision agriculture, Remote Sens. Environ. 90 (2004) 337–352, https://doi.org/10.1016/J.RSE.2003.12.013.
[54] A.A. Gitelson, Y.J. Kaufman, M.N. Merzlyak, Use of a green channel in remote sensing of global vegetation from EOS-MODIS, Remote Sens. Environ. 58 (1996) 289–298, https://doi.org/10.1016/S0034-4257(96)00072-7.
[55] R.P. Sripada, R.W. Heiniger, J.G. White, A.D. Meijer, Aerial color infrared photography for determining early In-season nitrogen requirements in corn, Agron. J. 98 (2006) 968–977, https://doi.org/10.2134/agronj2005.0200.
[56] A.A. Gitelson, A. Viña, T.J. Arkebauer, D.C. Rundquist, G. Keydan, B. Leavitt, Remote estimation of leaf area index and green leaf biomass in maize canopies, Geophys. Res. Lett. 30 (2003), https://doi.org/10.1029/2002GL016450.
[57] T. Ahamed, L. Tian, Y. Zhang, K.C. Ting, A review of remote sensing methods for biomass feedstock production, Biomass Bioenergy 35 (2011) 2455–2469, https://doi.org/10.1016/j.biombioe.2011.02.028.
[58] B. Datt, A new reflectance index for remote sensing of chlorophyll content in higher plants: tests using eucalyptus leaves, J. Plant Physiol. 154 (1999) 30–36, https://doi.org/10.1016/S0176-1617(99)80314-9.
[59] D. Haboudane, J.R. Miller, N. Tremblay, P.J. Zarco-Tejada, L. Dextraze, Integrated narrow-band vegetation indices for prediction of crop chlorophyll content for application to precision agriculture, Remote Sens. Environ. 81 (2002) 416–426, https://doi.org/10.1016/S0034-4257(02)00018-4.
[60] Q. Cao, Y. Miao, H. Wang, S. Huang, S. Cheng, R. Khosla, R. Jiang, Non-destructive estimation of rice plant nitrogen status with Crop Circle multispectral active canopy sensor, Field Crops Res. 154 (2013) 133–144, https://doi.org/10.1016/j.fcr.2013.08.005.
[61] M. Vincini, E. Frazzi, P. D'Alessio, A broad-band leaf chlorophyll vegetation index at the canopy scale, Precision Agric 9 (2008) 303–319, https://doi.org/10.1007/s11119-008-9075-z.
[62] G.A. Blackburn, Spectral indices for estimating photosynthetic pigment concentrations: a test using senescent tree leaves, Int. J. Remote Sens. 19 (1998) 657–675, https://doi.org/10.1080/014311698215919.
[63] R. Balaghi, B. Tychon, H. Eerens, M. Jlibene, Empirical regression models using NDVI, rainfall and temperature data for the early prediction of wheat grain yields in Morocco, Int. J. Appl. Earth Obs. Geoinf. 10 (2008) 438–452, https://doi.org/10.1016/j.jag.2006.12.001.
[64] F. Pedregosa, G. Varoquaux, A. Gramfort, V. Michel, B. Thirion, O. Grisel, M. Blondel, P. Prettenhofer, R. Weiss, V. Dubourg, J. Vanderplas, A. Passos, D. Cournapeau, M. Brucher, M. Perrot, É. Duchesnay, Scikit-learn: machine learning in Python, J. Mach. Learn Res. 12 (2011) 2825–2830. http://jmlr.org/papers/v12/pedregosa11a.html.
[65] N. Altman, M. Krzywinski, Simple linear regression, Nat. Methods 12 (2015) 999–1000, https://doi.org/10.1038/nmeth.3627.
[66] scikit-learn, DecisionTreeRegressor, Scikit-Learn (2025). https://scikit-learn.org/stable/modules/generated/sklearn.tree.DecisionTreeRegressor.html (accessed April 13, 2025).
[67] scikit-learn, RandomForestRegressor, Scikit-Learn (2025). https://scikit-learn/stable/modules/generated/sklearn.ensemble.RandomForestRegressor.html.
[68] scikit-learn, PolynomialFeatures, Scikit-Learn (2025). https://scikit-learn.org/stable/modules/generated/sklearn.preprocessing.PolynomialFeatures.html (accessed April 13, 2025).
[69] scikit-learn, SVR, Scikit-Learn (2025). https://scikit-learn.org/stable/modules/generated/sklearn.svm.SVR.html (accessed April 13, 2025).
[70] D. Gómez Fernández, R. Salas López, N.B. Rojas Briceño, J.O. Silva López, M. Oliva, Dynamics of the Burlan and Pomacochas Lakes using SAR data in GEE, machine learning classifiers, and regression methods, ISPRS Int. J. Geoinf. 11 (2022) 534, https://doi.org/10.3390/ijgi11110534.
[71] scikit-learn, r2_score, (2025). https://scikit-learn.org/stable/modules/generated/sklearn.metrics.r2_score.html#sklearn.metrics.r2_score (accessed April 13, 2025).
[72] Y. Takefuji, Beyond XGBoost and SHAP: unveiling true feature importance, J. Hazard. Mater. 488 (2025) 137382, https://doi.org/10.1016/J.JHAZMAT.2025.137382.
[73] X. Liu, X. Zhu, Y. Pan, S. Li, Y. Liu, Y. Ma, Agricultural drought monitoring: progress, challenges, and prospects, J. Geog. Sci. 26 (2016) 750–767, https://doi.org/10.1007/s11442-016-1297-9.
[74] INIA, Variedad de Arroz INIA 509 – Esperanza, (2010). https://hdl.handle.net/20.500.12955/1517 (accessed January 26, 2025).
[75] INIA, Nueva variedad de Arroz INIA 514 - Bellavista, (2018). https://hdl.handle.net/20.500.12955/1649 (accessed January 26, 2025).
[76] INIA, Nueva Variedad de Arroz para Costa Peruana INIA 513 – Puntilla, (2016). https://repositorio.inia.gob.pe/handle/20.500.12955/1119 (accessed January 26, 2025).
[77] INIA, Variedad de Arroz INIA 515 – Capoteña, (2020). https://hdl.handle.net/20.500.12955/1602 (accessed January 26, 2025).
[78] R.R. Barzan, H.A.S. Contreras, N.A.O. García, Nitrogen sources and rates in the initial growth of upland rice (Oryza sativa L.), Acta Agron 71 (2022) 405–409, https://doi.org/10.15446/ACAG.V71N4.92480.
[79] J.F. Caldas Cueva, A.Lizárraga Travaglini, Guía técnica: Manejo del Cultivo De Arroz Bajo Sistema De Riego Con Secas Intermitentes En Las Regiones De Tumbes, Piura, Lambayeque y Libertad, Instituto Nacional de Innovación Agraria, 2020. https://repositorio.inia.gob.pe/handle/20.500.12955/1053 (accessed March 14, 2025).
[80] D.P. Mullangie, K. Thiyagarajan, M. Swaminathan, J. Ramalingam, S. Natarajan, S. Govindan, Breeding resilience: exploring lodging resistance mechanisms in Rice, Rice Sci. 31 (2024) 659–672, https://doi.org/10.1016/J.RSCI.2024.08.002.
[81] H. Gu, Z. Xiao, Q. Meng, X. Fa, C. Wang, W. Jing, W. Wang, K. Zhu, W. Zhang, J. Gu, L. Liu, J. Zhang, H. Zhang, The synergistic effect of variety improvement and alternate wetting and drying irrigation on yield, water use efficiency and lodging resistance in rice, Eur. J. Agron. 164 (2025), https://doi.org/10.1016/J.EJA.2025.127507.
[82] J.Y. Barnaby, A.M. McClung, J.D. Edwards, S.R.M. Pinson, Identification of quantitative trait loci for tillering, root, and shoot biomass at the maximum tillering stage in rice, Sci. Rep. 12 (1) (2022) 1–13, https://doi.org/10.1038/s41598-022-17109-y, 202212.
[83] V. Vakeswaran, K. Rokini, M. Rajavel, Studies on tillering pattern in rice varieties, Int. J. Agric. Sci. 14 (2022) 11402–11405.
[84] T. Takai, Potential of rice tillering for sustainable food production, J. Exp. Bot. 75 (2024) 708–720, https://doi.org/10.1093/JXB/ERAD422.
[85] W. Zhou, F. Yan, Y. Chen, W. Ren, Optimized nitrogen application increases rice yield by improving the quality of tillers, Plant Prod Sci 25 (2022) 311–319, https://doi.org/10.1080/1343943X.2022.2061538.
[86] L. Yufei, H. Qun, Z. Yuxin, F. Dihui, F. Yuan, X. Fang, L. Guangyan, X. Zhipeng, G. Hui, W. Haiyan, Z. Hongcheng, Enhancing rice yield by optimizing tillering through transplantation of high-density seedlings cultivated on crop straw boards, J. Integr. Agric. (2025), https://doi.org/10.1016/j.jia.2025.02.048.
[87] E.I. Rhofita, R. Ouaret, L. Montastruc, M. Meyer, Mapping analysis of farmers' perceptions of rice straw valorization in Indonesia, Environ Dev 51 (2024) 101021, https://doi.org/10.1016/j.envdev.2024.101021.
[88] J. Zhang, L. Wan, C. Igathinathane, Z. Zhang, Y. Guo, D. Sun, H. Cen, Spatiotemporal heterogeneity of chlorophyll content and fluorescence response

within rice (Oryza sativa L.) canopies under different nitrogen treatments, Front. Plant Sci. 12 (2021) 645977, https://doi.org/10.3390/agronomy13010121.
[89] Semillas Potrero, Conociendo variedad HP 102 FL VALOR - YouTube, (2021). https://www.youtube.com/watch?v=hteZLU2iq48&t=84s (accessed January 26, 2025).
[90] A. Paiman, C.T. Kusumastuti, S. Gunawan, F. Ardiani, Maximizing the rice yield (Oryza Sativa L.) using NPK fertilizer, Open Agric J 15 (2021) 33–38, https://doi.org/10.2174/1874331502115010033.
[91] P. Negi, J. Rane, R.S. Wagh, T.J. Bhor, D.D. Godse, P. Jadhav, C. Anilkumar, D. Sreekanth, K. Sammi Reddy, S.R. Gadakh, K.M. Boraih, C.B. Harisha, P. S. Basavaraj, Direct-seeded Rice: genetic improvement of game-changing traits for better adaption, Rice Sci. 31 (2024) 417–433, https://doi.org/10.1016/j.rsci.2024.04.006.
[92] W. Chouari, Assessment of vegetation cover changes and the contributing factors in the Al-Ahsa Oasis using normalized Difference Vegetation Index (NDVI), Regional Sustainability 5 (2024), https://doi.org/10.1016/j.regsus.2024.03.005.
[93] V.J. Melino, M.A. Tester, M. Okamoto, Strategies for engineering improved nitrogen use efficiency in crop plants via redistribution and recycling of organic nitrogen, Curr. Opin. Biotechnol. 73 (2022) 263–269, https://doi.org/10.1016/j.copbio.2021.09.003.
[94] T. Xu, F. Wang, Z. Shi, Y. Miao, Multi-scale monitoring of rice aboveground biomass by combining spectral and textural information from UAV hyperspectral images, Int. J. Appl. Earth Obs. Geoinf. 127 (2024), https://doi.org/10.1016/j.jag.2024.103655.
[95] J. Xue, B. Su, Significant remote sensing vegetation indices: a review of developments and applications, J. Sens. 2017 (2017) 1353691, https://doi.org/10.1155/2017/1353691.
[96] M. Hossain, H.M. Abdullah, T. Ahmmed, M.G. Miah, M.U. Salam, M. Islam, M. M. Rahman, Quantifying canopy nitrogen of Aman rice utilizing multi-temporal unmanned aerial systems, Remote Sens. Appl. 34 (2024), https://doi.org/10.1016/j.rsase.2024.101141.
[97] S. Snehi, R.K. Kt, S. Rathi, S. Upadhyay, S. Kota, S.K. Sanwal, L. Bm, A. Balasubramaniam, N.R. Prakash, P.K. Singh, Discerning genes to deliver varieties: enhancing vegetative and reproductive stage flooding tolerance in rice, Rice Sci. (2025), https://doi.org/10.1016/j.rsci.2025.01.002.
[98] Q. Su, J.S. Rohila, S. Ranganathan, R. Karthikeyan, Rice yield and quality in response to daytime and nighttime temperature increase – A meta-analysis perspective, Sci. Total Environ. (2023), https://doi.org/10.1016/J.SCITOTENV.2023.165256.
[99] B. Sánchez, A. Rasmussen, J.R. Porter, Temperatures and the growth and development of maize and rice: a review, Glob. Chang. Biol. 20 (2014) 408–417, https://doi.org/10.1111/GCB.12389.
[100] P.V.V. Prasad, K.J. Boote, L.H. Allen, J.E. Sheehy, J.M.G. Thomas, Species, ecotype and cultivar differences in spikelet fertility and harvest index of rice in response to high temperature stress, Field Crops Res. 95 (2006) 398–411, https://doi.org/10.1016/J.FCR.2005.04.008.
[101] M. Liu, Y. Zhou, J. Sun, F. Mao, Q. Yao, B. Li, Y. Wang, Y. Gao, X. Dong, S. Liao, P. Wang, S. Huang, From the floret to the canopy: high temperature tolerance during flowering, Plant Commun 4 (2023), https://doi.org/10.1016/J.XPLC.2023.100629.
[102] Y.C. Su, B.J. Kuo, Risk assessment of rice damage due to heavy rain in Taiwan, Agriculture 13 (2023) 630, https://doi.org/10.3390/AGRICULTURE13030630.
[103] J. Yu, T. Du, P. Zhang, Z. Ma, X. Chen, J. Cao, H. Li, T. Li, Y. Zhu, F. Xu, Q. Hu, G. Liu, G. Li, H. Wei, Impacts of high temperatures on the growth and development of rice and measures for heat tolerance regulation: a review, Agronomy 14 (2024), https://doi.org/10.3390/agronomy14122811.
[104] D.H. Wu, C.T. Chen, M. Der Yang, Y.C. Wu, C.Y. Lin, M.H. Lai, C.Y. Yang, Controlling the lodging risk of rice based on a plant height dynamic model, Bot. Stud. 63 (2022) 1–12, https://doi.org/10.1186/s40529-022-00356-7.
[105] J. Dagnino, Comparaciones múltiples, Revista Chilena de Anestesia 43 (2014). https://revistachilenadeanestesia.cl/comparaciones-multiples/ (accessed March 15, 2025).
[106] Z. Wei, Y. Zhang, W. Jin, Yield gap analysis of super high-yielding rice (>15 t ha−1) in two ecological regions, Agric. (Switzerland) (2024) 14, https://doi.org/10.3390/agriculture14030491.
[107] John K. Saichuk, C.A. Hollier, S. Brown, E.P. Webster, B. Schultz, L.M. White, J. H. Oard, D.L. Harrell, D.E. Groth, S.D. Linscombe, M. Salassi, M. Stout, Rice Production Handbook, 2015. https://www.lsuagcenter.com/portals/communications/publications/publications_catalog/crops_livestock/rice/rice-production-handbook1 (accessed March 15, 2025).
[108] L. Freijeiro-González, M. Febrero-Bande, W. González-Manteiga, A critical review of LASSO and its derivatives for variable selection under dependence among covariates, Int. Statist. Rev. 90 (2022) 118–145, https://doi.org/10.1111/insr.12469.
[109] A. Amiri-Simkooei, C. Tiberius, R. Lindenbergh, Deep learning in standard least-squares theory of linear models: perspective, development and vision, Eng. Appl. Artif. Intell. 138 (2024), https://doi.org/10.1016/J.ENGAPPAI.2024.109376.
[110] N. Dominic, T.W. Cenggoro, B. Pardamean, Systematic literature review on statistics and machine learning predictive models for Rice phenotypes, Procedia Comput. Sci. 227 (2023) 1054–1061, https://doi.org/10.1016/J.PROCS.2023.10.615.